Publication No. WI-2016-02

28 January 2016

The Watershed Institute

Division of Science and Environmental Policy

California State University Monterey Bay

http://watershed.csumb.edu

100 Campus Center, Seaside, CA, 93955

Central Coast Watershed Studies

CCoWS

Sediment Trapping Function of an Unmanaged Fluvial Wetland: Carneros Creek, Monterey County

Douglas Smith, PhD
Ryan Bassett
Randy Holloway
John Silveus
Kaitlyn Chow
Lauren Luna
Shaelyn Hession
Polly Perkins
Fred Watson
Bryan Largay
Amelia Olson

Lead Author Contact: dosmith@csumb.edu

Acknowledgements

- U.S. EPA funded this project
- CSUMB UROC provided student researchers
- Kaley Grimland managed the broad project that this study supports
- Many CSUMB students volunteered as field assistants on this project

This report may be cited as:

Smith D., Bassett R., Holloway R., Silveus J., Luna L., Chow K., Hession S., Perkins P., Watson F., Largay, B., and Olson, A. 2015. Sediment Trapping Function of an Unmanaged Wetland: Carneros Creek, Monterey County. The Watershed Institute, California State Monterey Bay, Publication No. WI-2016-02, 69pp.

Executive Summary

In 1998 a series of strong winter storms triggered slope failure adjacent to the channelized Carneros Creek channel, downstream of the Triple M Ranch property. The resulting channel occlusion forced the channel to avulse through a poorly-engineered levee on Triple M Ranch. The redirected flow restored wetland hydrology to a section of the floodplain that had been historically used for agriculture. The unmanaged site rapidly converted to a smartweed marsh. In 2013 several ponds and mounds were constructed in the marsh to improve amphibian habitat.

In 2009, the CSUMB Watershed Geology Lab was engaged to monitor the sediment trapping function of the complex, unmanaged wetland system in a period that spanned before and after pond construction. While the principle focus of this study was to assess the differences in sediment trapping with, and without, ponds, the project had four general goals during the 6 year study: 1) understanding ALBA wetland flow patterns and wetland characteristics, 2) measuring the sediment trapping efficiency of the ALBA wetlands, 3) predicting the ALBA wetland function in assumed future climate and watershed land-use conditions, and 4) developing a conceptual design for stream channel restoration on ALBA property, if more efficient sediment transport became a desired management option for Elkhorn Slough.

The flow patterns in the unmanaged wetland are complex, governed in part by pre-existing field-bounding ditch system and flow access to a northern and southern wetland, located on opposite sides of the occluded channel. Therefore, the residence time of any slug of sediment-laden water is very hard to predict. During a dye-tracing study, residence time varied from 3 hr to 28 hr, and varied inversely proportional to the discharge. Sedimentation patterns were governed by distance from the wetland inlet, vegetation density, and vegetation type (smartweed vs. reeds). A map of sediment deposits based upon turf mats shows the presence of a growing crevasse splay deposit in the southern wetland and a smaller sediment fan at the entry to the northern wetland.

We rated stream gages for suspended sediment both upstream and downstream of the wetlands from 2010 to 2015, excluding 2013. Annual sediment trapping of the wetlands ranged from 12 tonnes to 2611 tonnes, with a range of trapping efficiency from 46% to 86% of the sediment that entered the wetlands. There was no

discernable difference in trapping efficiency before and after the ponds were constructed. Bedload composed approximately 1% of the sediment entering the property, and is generally trapped upstream of the wetlands.

Various topographic survey strategies were unable to detect annual topographic changes in the wetland topography from sediment deposition or erosion. In the last year the pond bottoms filled an average of 0.03 m with sediment.

Climate models indicate that the Carneros watershed will have longer dry seasons, and a shorter winter with fewer, but more intense, storms. Based upon the literature, sediment yield and sediment transport will increase. Sediment trapping is a function of residence time, and residence time is inversely related to discharge, so increased storm intensity is forecast to reduce the sediment trapping efficiency of the wetlands.

San Benito County does not have specific buildout densities for the watershed, but the plan language is supportive of low impact development. The general plan for Monterey County includes increased housing density for the watershed, with 1 house/5 ac density increasing to 1 to 5 houses / ac on buildable lots, but stopping short of stressing the existing sewer system. While we do not know how much impervious cover will increase as a function of the housing density change, our modeling indicates that an increase from the current 4% impervious cover to 10% impervious cover will increase peak discharge by 10% and runoff volume by 5%. The resulting increase in impervious cover could lead to increases peak discharge, which would decrease sediment trapping efficiency of the wetlands.

We present a conceptual design for an appropriately-scaled channel and floodplain system that can be considered in future resource management decisions.

Table of Contents

1 Introduction

The 195 acre Triple M Ranch is located near the mouth of Carneros Creek, the largest tributary feeding the Elkhorn Slough (Figure 1). In this key position, the property is virtually the last parcel that can either pass, or retain, sediment derived from the entire watershed. Recently-created, broad fluvial wetlands on the Ranch serve to trap an unknown quantity of sediment that would otherwise be transported to the Slough.

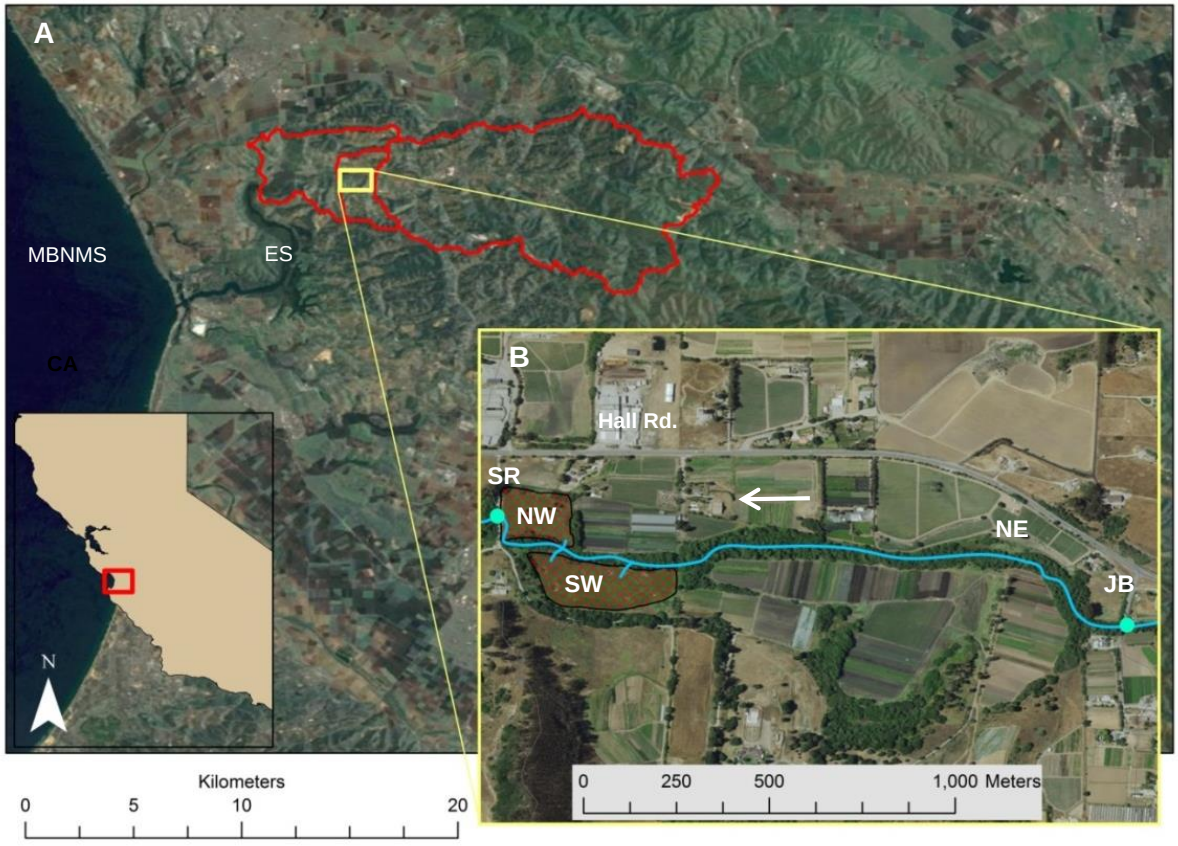

Figure 1: Study Location. A) Yellow box is the position of the Triple M Ranch within the Carneros Creek watershed (red outline), just upstream from the Elkhorn Slough (ES), which is fully connected to the Monterey Bay National Marine Sanctuary (MBNMS). B) The study area in Las Lomas, CA includes the Carneros Creek channel (blue line) located between the Johnson Bridge stream gage (blue dot near JB) and the stream gage at Sill Road (blue dot near SR). Checked pattern shows the locations of broad riparian wetlands formed by avulsion in 1998. The wetlands are separated into norther wetlands (NW) and southern wetland (SW). Arrow shows the down-valley direction.

The wetlands located on the Ranch are "self-restored" wetlands that formed when sediment blocked the main flood canal draining the property. Carneros Creek was channelized throughout much of its watershed during the last century to promote

farming and urban growth in fluvial floodplain settings (Largay 2007). Riverside farming on Triple M Ranch was made possible by flood protection afforded by the flood canal and attendant ridge of dredge spoils that form rudimentary "levees" against flood waters. The canal was intended to convey flood waters past the Ranch to Porter Marsh, the first waters of Elkhorn Slough. Extreme weather in 1998 led to slope failure that plugged the canal just downstream from the Triple M Ranch (Largay 2007; Fig. 2).

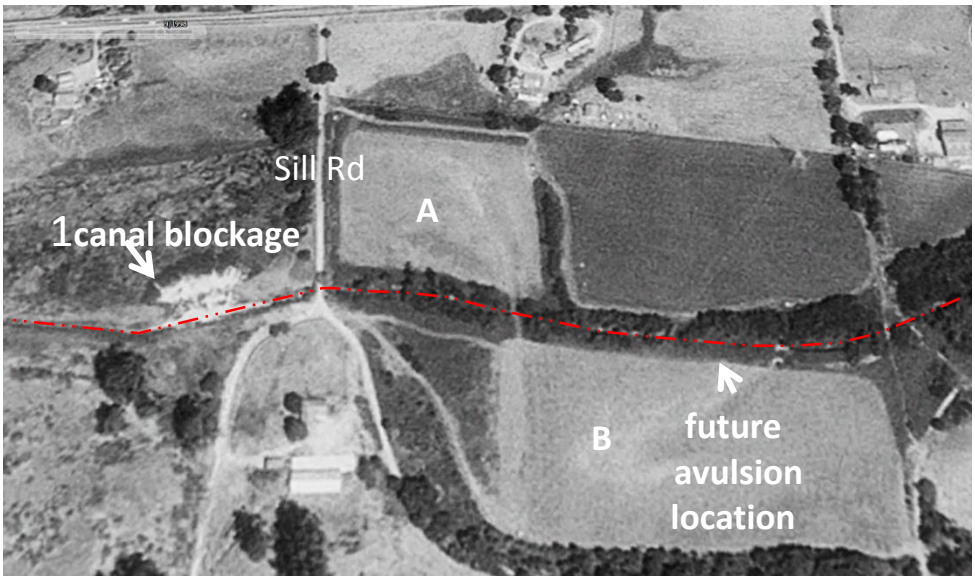

Figure 2: In 1998, storm-triggered slope failure brought sediment into and across the Carneros Creek channel (red) downstream (left) of Sill Rd. Backwater behind the blockage broke through the levee. Flow through the levee breech has maintained wetland hydrology in the northern (A) and southern (B) wetlands since that time. Google Earth 1998 image.

Backwater from the plug forced the canal to avulse into the tilled fields of Triple M Ranch, instantaneously creating the wetlands by restoring slowly-drained wetland hydrology to 13 acres (5.3 hectares) of previously arable land (Largay 2007). This process of "self restoration" has been well-documented in other watersheds where channelized, low-gradient valleys cannot transport sand supplied from sand-laden tributaries (Smith et al. 2009).

Triple M Ranch is managed by the Agriculture and Land Based Training Association (ALBA). ALBA has the combined goals of promoting and training farmers in sustainable agriculture, as well as preserving and restoring natural habitat and ecosystem functions on the Ranch. To enhance the ecosystem function of the property, several ponds and low hills were constructed to provide more habitat diversity in the new fluvial wetlands (ALBA wetlands). Our study assessed how the floodplain modifications influenced the sediment trapping function of the wetlands. We also provided insight

about how both climate change and watershed land-use change might influence the future sediment trapping function of the wetlands. Lastly, we developed a preliminary channel design in case future resource managers decide to restore a more naturally-functioning fluvial system on the property.

1.1 Carneros Creek Watershed Characteristics

1.1.1 Physical and Cultural Landscape

The physiography of the portion of the Carneros Creek that feeds water and sediment to the Triple M Ranch is characterized in Table 1.

Table 1: Carneros Creek watershed geometry upstream of Triple M Ranch

	Metric	English
Drainage Area	60 km^2	24 mi^2
Aspect	west	west
Min elevation	5 m	15 ft
Max elevation	400 m	1300 ft
Mean elevation	116 m	380 ft
Relief	390 m	1290 ft
Length	13,110 m	43,000 ft
Average Slope	0.03	0.03

The watershed geology is dominated by easily eroded Quaternary sand dune deposits (Qa; Figure 3) and creeping regolith (Qc; Figure 3). The soil mantling the watershed is divided into sandy, well drained soils on the side slopes (Fig. 4, Group B) and poorly drained clayey floodplain soils in the bottoms (Fig. 4, Groups C and D). Two dominant soils on the Triple M Ranch include Aquic Xerofluvents and Clear Lake clay. Aquic Xerofluvents is found in areas with channels and floodplains while Clear Lake clay is found in areas with still water such as estuaries and wetlands. Permeability is low due to a high clay content which is typical for estuary soils (Soil Conservation Service 1978).

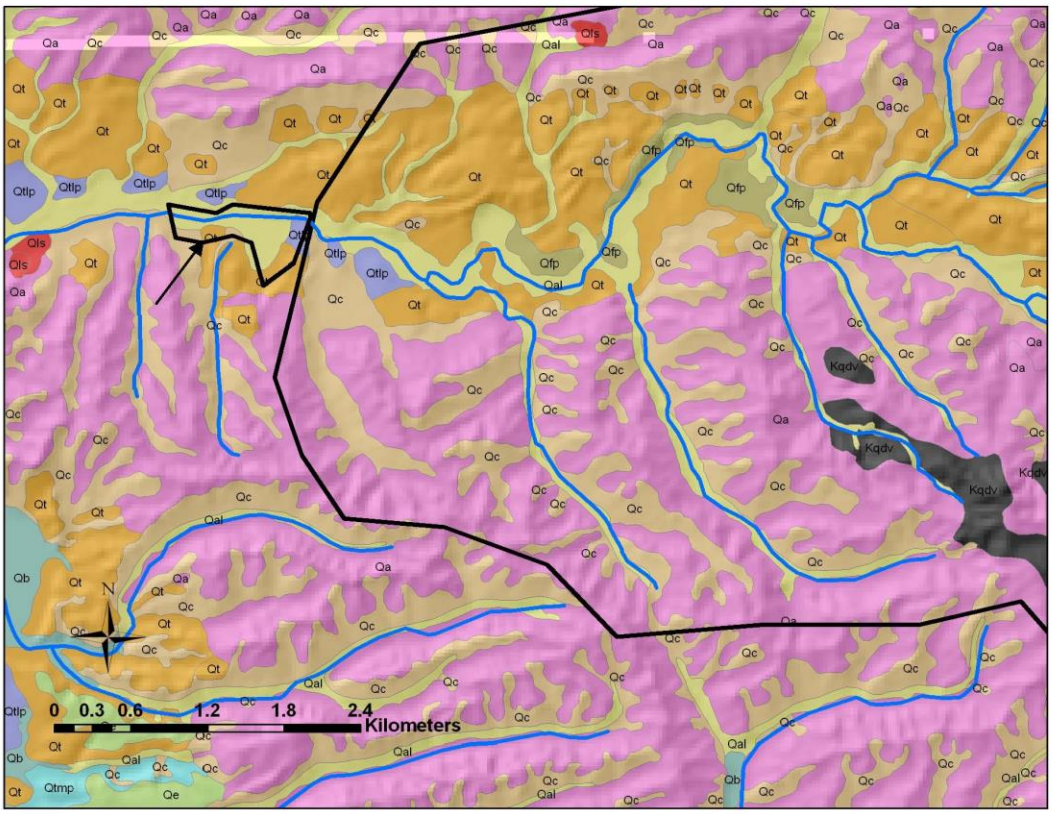

Figure 3. Geologic units exposed in lower Carneros Watershed. Black line is the boundary of the watershed region immediately up valley from Triple M Ranch (arrow). The watershed substrate is chiefly old sand dune deposits of the Aromas Fm. (Qa), Fluvial terrace deposits (Qt), and Colluvial soils derived from the previous two units (Qc). Ancillary units are Cretaceous "granitic" rocks (Kqdv) and modern stream deposits (Qal). Data from Rosenberg (2001).

The soil series and bedrock formations of the watershed are relatively young and poorly lithified, so they are highly susceptible to erosion. Figure 5 shows typical erosion potential in the watershed, with an abundance of red zones indicating high erosion risk. Land use in the Carneros Creek watershed also contributes to excessive erosion and flashy runoff. A significant portion of the watershed is devoted to strawberry farming, and the plastic mulch used for this crop acts as an impervious surface (Largay 2007). Rainfall is funneled into gullies, and large storm events can release massive amounts of sediment. Greenhouses in the watershed function hydrologically as suburban pavement, enabling rainfall to quickly run off without saturating the ground. These impervious surfaces result in higher peak floods and more erosion (Largay, 2007).

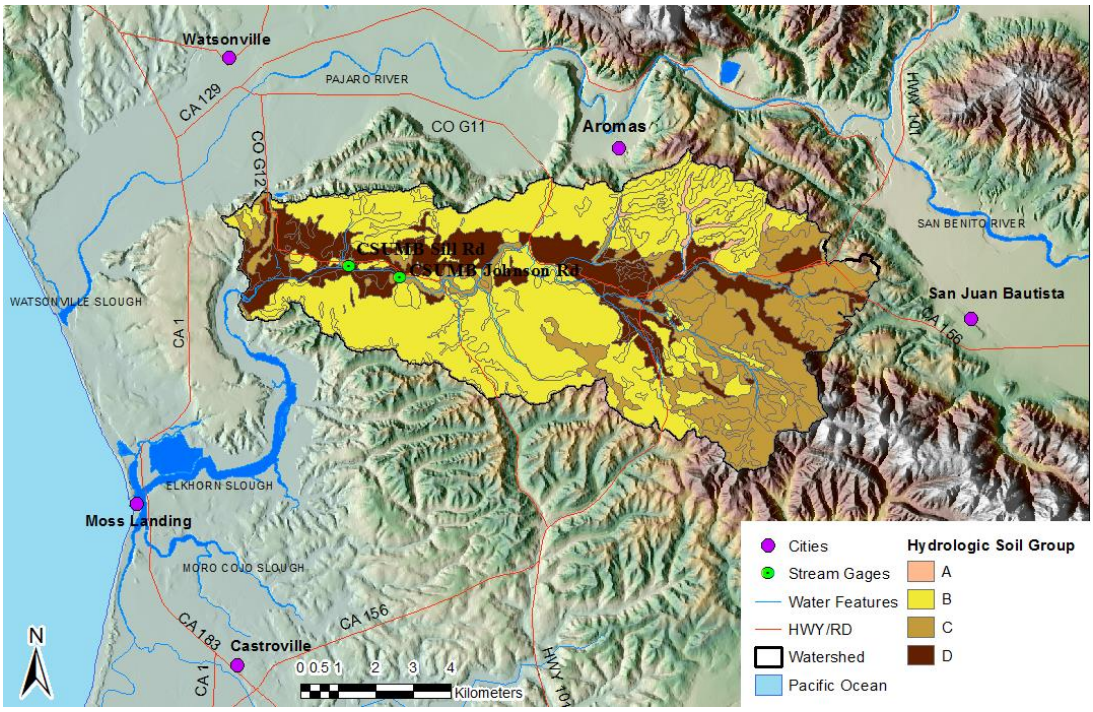

Figure 4. Hydrologic soil groups of the Carneros Watershed. Data from SSURGO 2012.

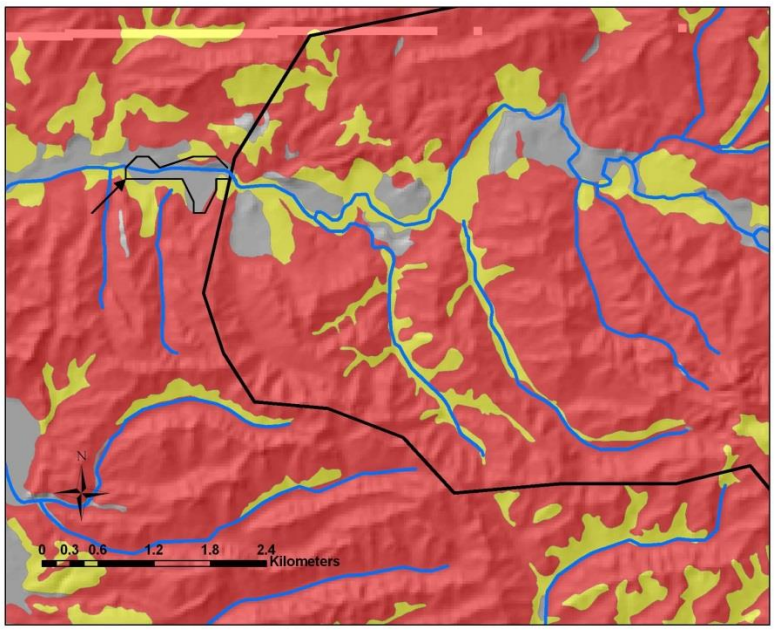

Figure 5: Erosion susceptibility in lower Carneros Watershed. Red is high susceptibility, yellow is moderate, grey is low. Black line is the boundary of the watershed region immediately up valley from Triple M Ranch (arrow). Data from Rosenberg (2001).

The watershed land is used in a variety of ways, including agriculture, grazing, rural development, mining, and undeveloped areas (USDA 2006; Fig. 6). Approximately 2% of the watershed area is taken up by crops such as berries, flowers, and mixed vegetables. Another 28% is developed land that ranges from low to high intensity. The remaining 70% is largely undeveloped land containing grasslands, oak woodland, maritime chaparral, and riparian woodland (Elkhorn Slough National Estuarine Research Reserve, 2007). The Carneros watershed spans two counties, Monterey (71%) and San Benito (29%), both having similar land use regulations which value conservation. The watershed is still largely rural, with only 4% impervious cover at this time (Fig. 7). This report addresses the potential impact of future urbanization on the ALBA wetland hydrology and sediment retention.

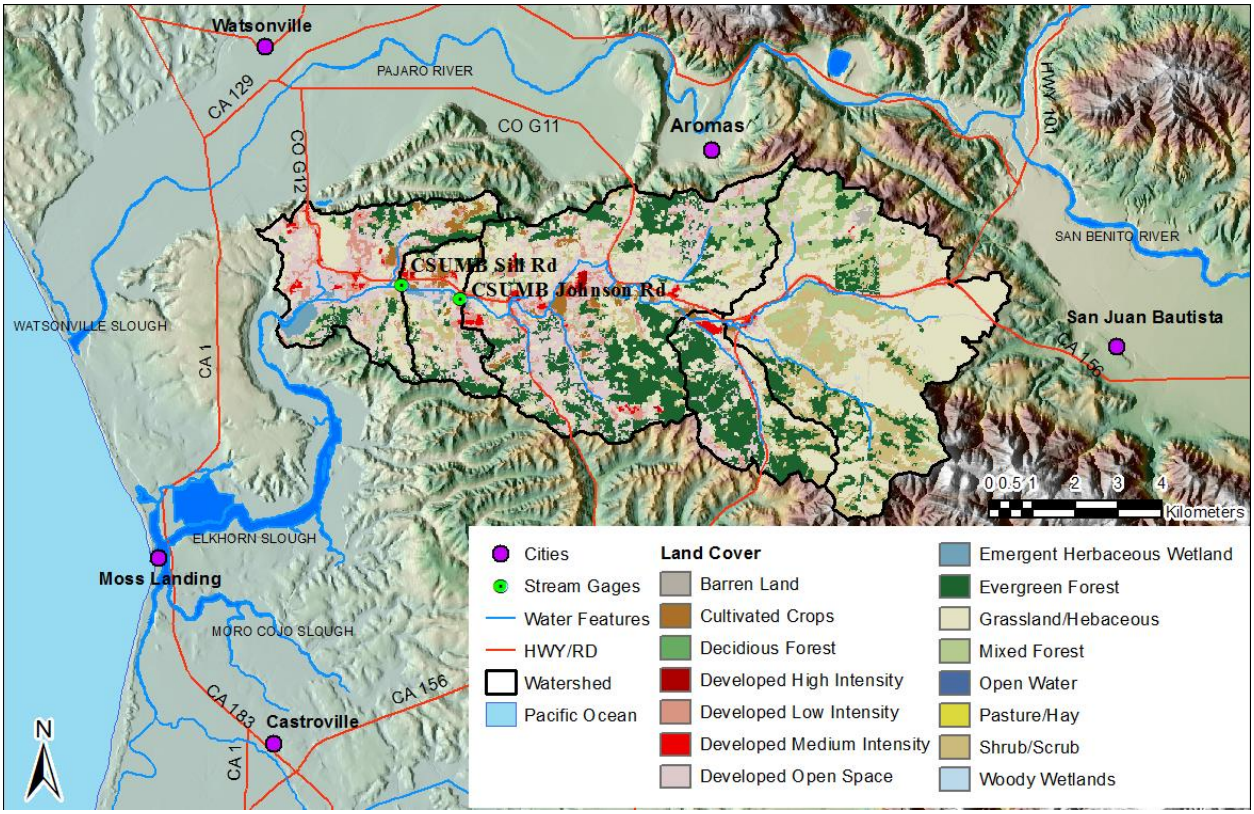

Figure 6: Land use in the Carneros Watershed. Data from 2006 USGS National Land Cover Database.

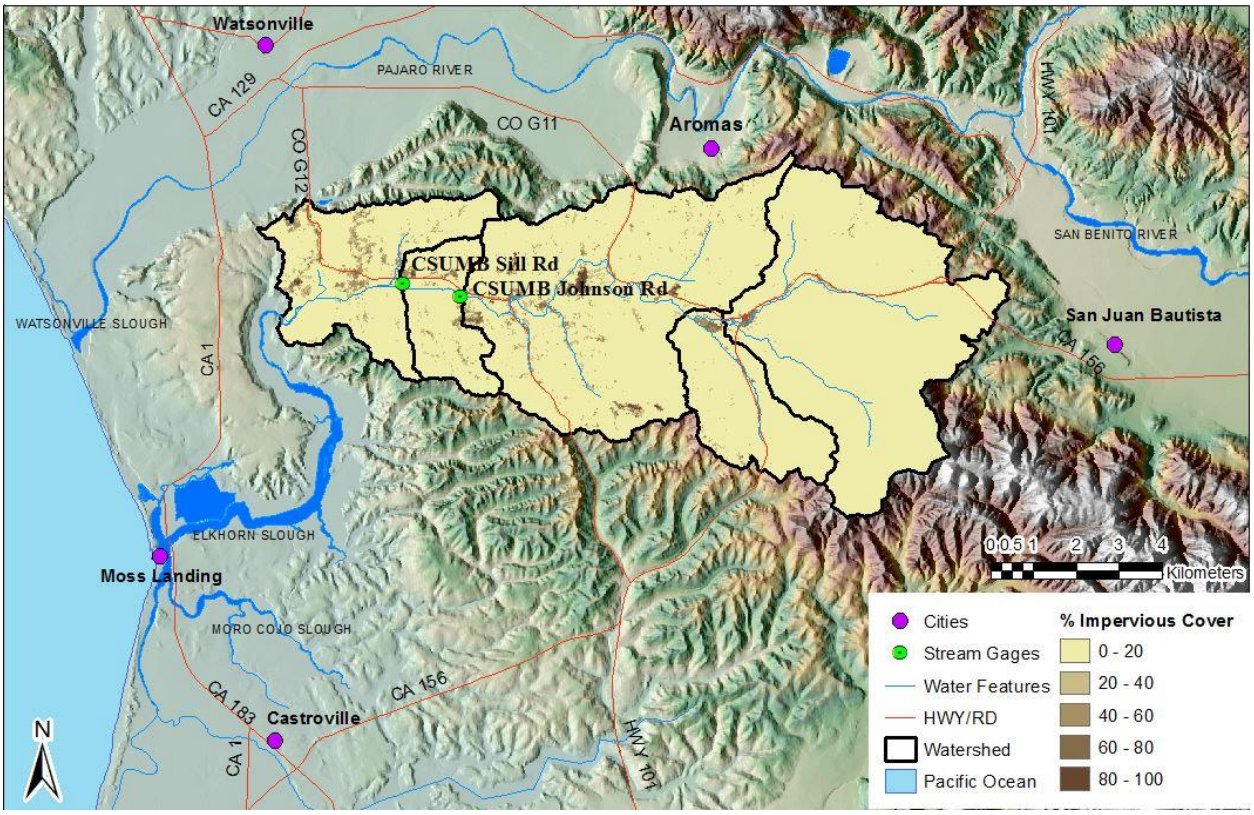

Figure 7: Distribution of imperious cover in the Carneros Watershed. Overall, the watershed has approximately 4% imperious cover. Data from 2006 USGS National Land Cover Database.

1.1.2 Climate and Hydrology

The Carneros watershed has a Mediterranean climate with cool winters, mild summer temperatures, and a high evaporation rate. Average annual temperatures typically range from 50 F to 61 F (Weatherbase 2015). The watershed receives 45.7 cm/yr average precipitation (Laurel Marcus & Associates 2003; Fig. 8), typically delivered in four to ten frontal storms between October and March. Average runoff volume is approximately 2,800 acre-feet per year (Raines, Mellon and Carella, Inc. 2002). The stream also carries extreme floods during decadal-scale El Nino events.

Carneros Creek is an annual stream with no summer flow. The groundwater basin in this area is under acute overdraft (Raines, Mellon and Carella Inc. 2002), but the study wetlands are separated from the aquifer by a thick confining clay layer located in the shallow subsurface.

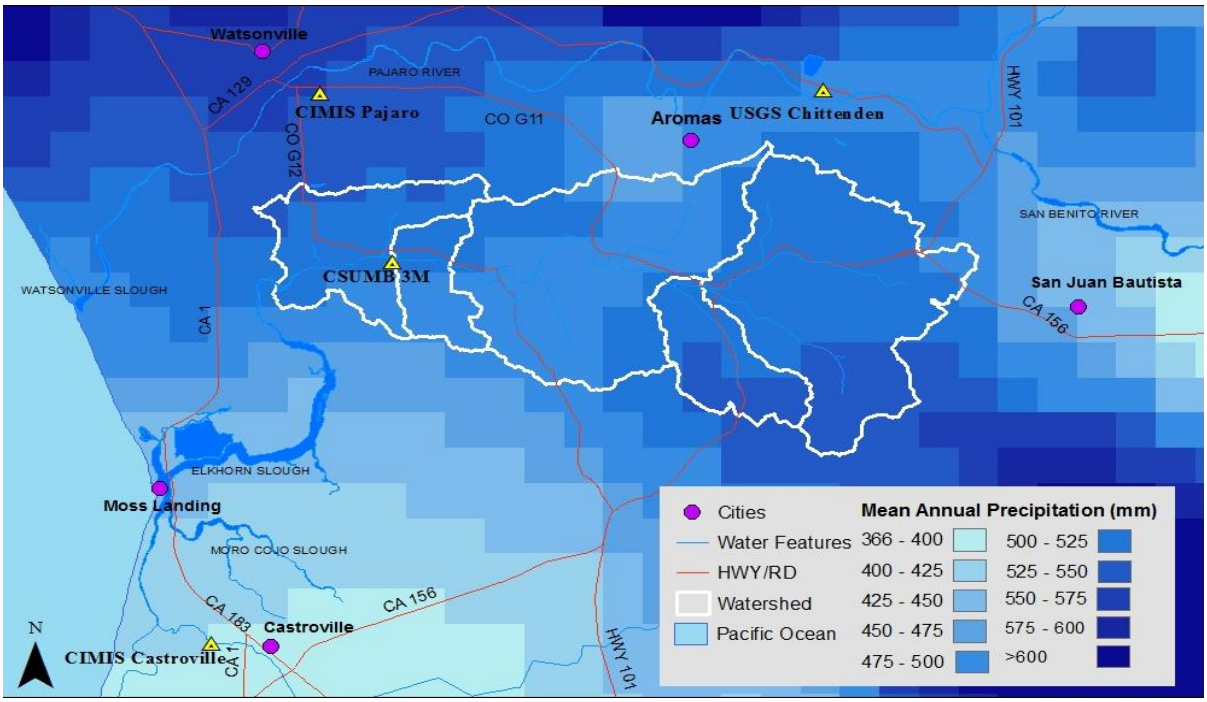

Figure 8. Carneros watershed average annual precipitation, 1981-2010 (PRISM 2012).

1.1.3 ALBA Wetlands

Tripe M Ranch includes three principle areas of sediment retention: northeast floodplain, northern wetland, and southern wetland (Fig. 1). The northeast floodplain is a 1.3 ha parcel that is located at the upstream entrance to the property. Prior to the study, this narrow floodplain was cropland until it was buried by a great volume of sediment delivered to the site by high magnitude El Nino floods of 1997-98. That sediment was graded flat prior to the study, leaving a barren sandy surface. During the study, the northeast floodplain continued to aggrade during minor flood events (Bassett, 2010). The parcel was not used for agriculture thereafter, and eventually became a dense willow forest.

Water flowing downstream from the northeast floodplain slows and deepens before spilling south through an avulsion channel. Backwater from the avulsion forces bedload deposition in the channel and northeast floodplain. Water flowing through the avulsion channel immediately slows as it enters standing water of the southern wetland. The sudden flow deceleration has produced a crevasse splay (depositional sediment fan) at the mouth of the avulsion channel (Fig. 9).

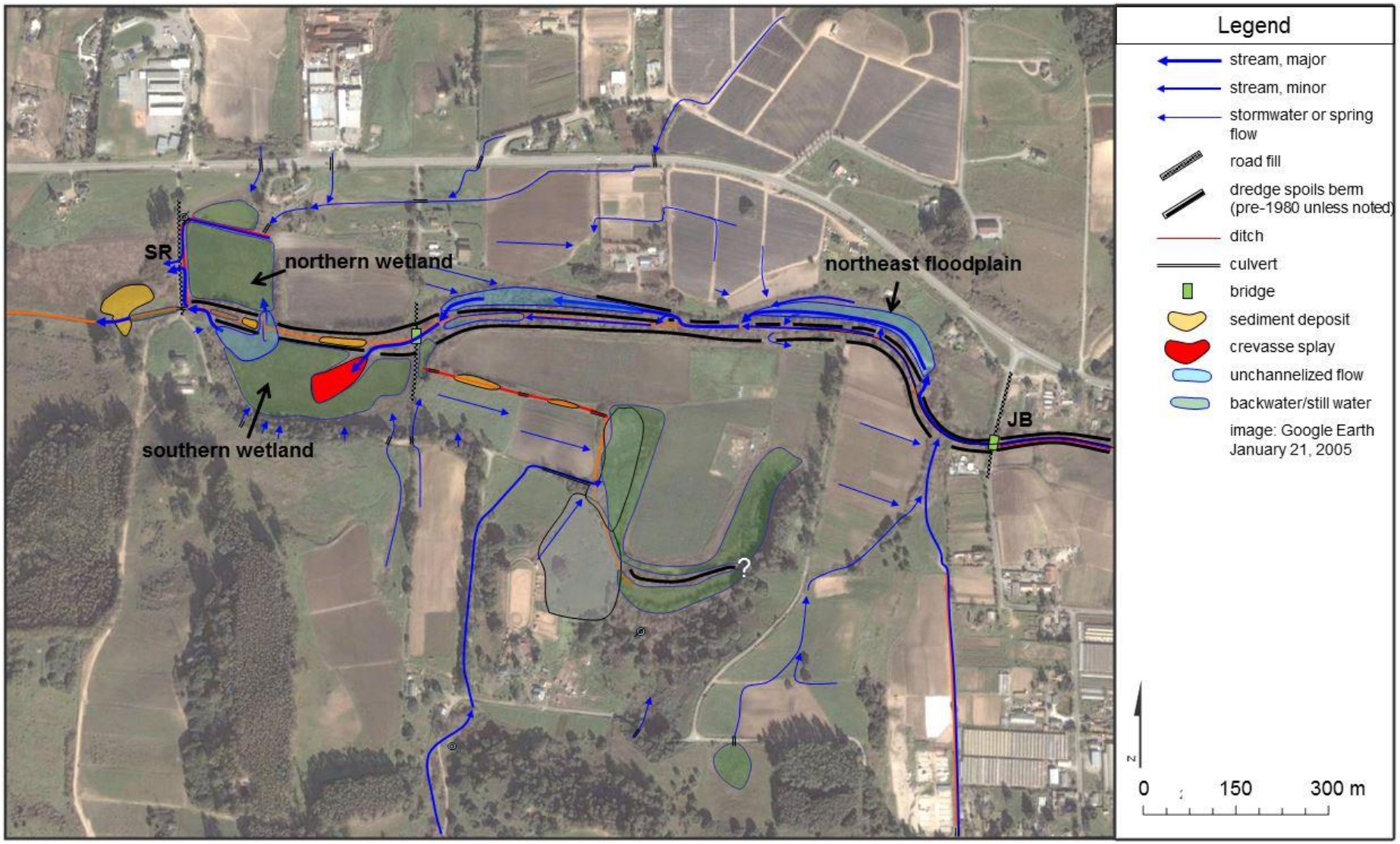

Figure 9: General features and flow pathways of the Triple M Ranch. The study area includes the northeast floodplain and ALBA wetlands (northern and southern wetlands). JB and SR are the Johnson Bridge and Sill Road gage locations. Modified from Largay (2007).

Water flows from the southern wetland to the northern wetland through one of two narrow gaps in the levees, and then traverses the northern floodplain either in field-bounding drainage ditches, or across the floodplain surface, depending upon flow depth (Fig. 9). At the start of the project in 2009 the exit from the northern wetland was across a broad ford in Sill Road (Fig. 10).

Figure 10: Ford across Sill Road was the downstream end of stream flow through Tripe M Ranch. Photo from 2009. View to the south. Flow from left to right.

In 2012 Sill Road was reconstructed to accommodate a three-box concrete culvert (Fig. 11a). Moderate flows still top the culvert and flow across the road surface (Fig 11b). A large culvert located in the abandoned Carneros channel can be opened to divert flood flow, which would reduce the frequency of road-topping flows

Approximately 15 shallow ponds were excavated in many areas of the Triple M Ranch in 2012 to provide habitat for native amphibians (Santa Cruz long-toed salamander, tiger salamander, and red-legged frog), and to improve water quality by trapping sediment. To further increase habitat diversity, the soil excavated from each pond was mounded adjacent to the pond to increase the elevation span in the wetland setting. Ten of the ponds were excavated in the northern and southern wetlands and are part of the present study (Fig. 12).

The ALBA Wetlands currently cover 22 ha, with 9 ha distributed in two marsh fields at the lower end of the site, 4 ha in the floodplains, and 9 ha in channel and riparian corridor. Typical vegetation found on the site is willow (*Salix sp.*), blackberry, and central coast scrub along the floodplain. The marsh area contains smartweed (*Polygonum amphibium*), cattails, and hemlock (*Conium maculatum*) (Fig. 13).

Figure 11: A) New box culvert beneath Sill Road. The white rectangle in the center of the picture is a staff plate. Black cylinder on the right side of the image is the stilling well for the pressure transducer of the Sill Road gage (Fig. 8). B) Same view as Figure 9 during 12/12/15 flow of 2014. Flow rate is approximately 90 cfs, corresponding to an exceedance recurrence interval of less than 0.5 years.

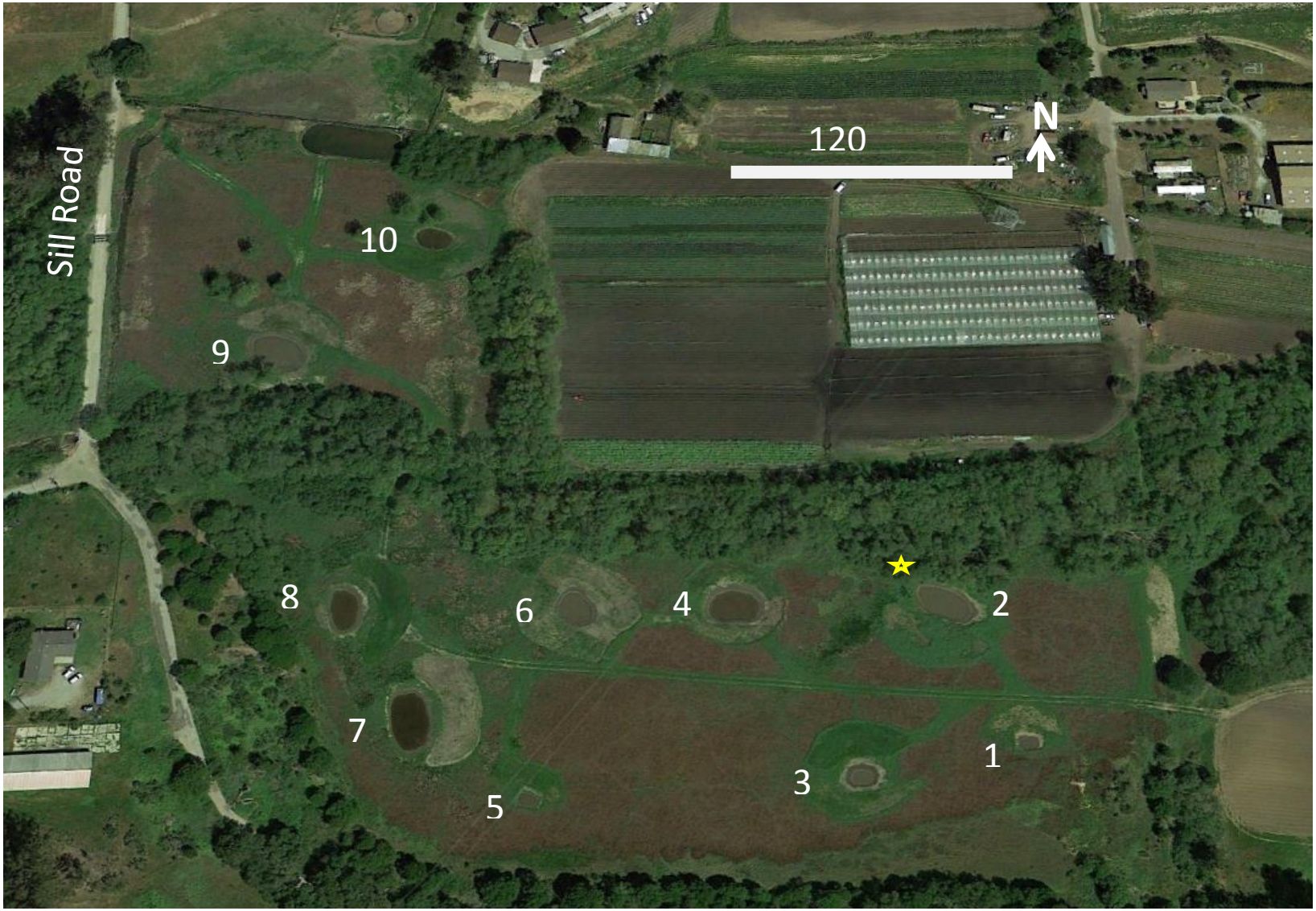

Figure 12: Ten ponds and mounds were constructed in the ALBA wetlands for habitat improvement in 2012. Yellow star is avulsion point where channelized flow meets unchannelized wetland hydrology. Google image 2013.

Figure 13: Broad expanse of smartweed in the northern wetland in summer 2015.

1.2 Goals

The goals of this study fall into four main areas: 1) understanding ALBA wetland flow patterns and wetland characteristics, 2) measuring the sediment trapping efficiency of the ALBA wetlands, 3) predicting the ALBA wetland function in assumed future climate and watershed land-use conditions, and 4) developing a conceptual design for stream channel restoration on ALBA property, if more efficient sediment transport became a desired management option for Elkhorn Slough.

The ALBA wetlands comprise a complex network of channels and floodplains that in turn leads to complex hydrology and sediment response. Our first goal was to develop a more accurate understanding of residence time, water pathways, and general sedimentation patterns. We used surveys, dye tracing, and sediment traps in this phase of the study.

The second goal of this project was to determine if pond construction changed the sediment retention function of the wetland. This part of the study focused on measuring sediment movement on an annual basis.

We explored the potential future sediment trapping efficiency of the ALBA wetland in the context of future climate change and urbanization. This goal was met in part by watershed modeling and in large part by a review and synthesis of current literature.

Elkhorn Slough is out of balance between terrestrial and marine influences. The low-lying estuarine landforms are being eroded faster than deposition can rebuild them. It is possible that additional sediment from the Carneros watershed could partially mitigate that imbalance. If resource managers were interested in maximizing sediment transport to the Slough, an option would be to construct a more natural channel-floodplain system across the ALBA property where sediment is currently being trapped. Our last goal was to develop a preliminary design for that channel-floodplain system using natural channel design principles.

2 Methods

2.1 ALBA Wetland Flow Dynamics.

General flow paths through the Triple M Ranch were well documented by Largay (2007; Fig. 9); they were also observed during the present study via visual inspection during flow events, and by assessment of the spatial distribution of sediment deposits following storm runoff. Stormwater residence time in the wetlands downstream of the avulsion point (southern and northern wetlands) was assessed in water year 2010. Spatial patterns of sedimentation, and their causes were assessed in water year 2012 through turf mat trapping, whose methods are described below in section 2.2.3.

2.1.1 Residence Time

Hydraulic time of travel was measured through the downstream marsh fields by slug dye- tracer experiments (Holland et al. 2004; Kadlec and Knight 1996; Kilpatrick and Wilson 1989; Stern et al. 2001). Slug dye experiments were performed 6 times, once from Johnson Bridge to Railcar Bridge, once from Johnson to Sill, and five times from Railcar Bridge to Sill Rd. The dates of the experiments were 1/29/2010, 2/6/2010, 2/11/2010, 2/24/2010, 3/9/2010, and 3/23/2010 respectively. An in situ fluorometer (Model C3, Turner

Corporation) measured fluorescence from passing dye concentrations every 30 seconds at Sill Road.

The fluorometer record resulted in a residence time distribution for each experiment. The residence time distribution (RTD) consists of the fluorescence weighted by discharge at the time of measurement graphed versus time from injection of the dye upstream. Weighting of the fluorescence record by discharge was through multiplying fluorescence in Relative Fluorescence Units by discharge in m^3s^{-1}. Fluorescence could not be converted to concentration due to differences in the background levels present in laboratory calibration and actual background levels in the field. Starting dye dosage was initially calculated using the formula from Kilpatrick and Wilson (1989) and then adjusted to achieve desired signal strength. The times to leading edge, peak, centroid, and trailing edge were determined. Time to leading edge was calculated as the time to a concentration equal to 3% of the peak concentration (Holland et al. 2004), while the trailing edge was time to 10% of the peak concentration (Kilpatrick and Wilson 1989). The residence time was the time to centroid, calculated as the time to one-half of the area under the curve given by the residence time distribution (Holland et al. 2004).

Background fluorescence was measured for one or more hours immediately prior to dye introduction (Stern et al. 2001). To adjust for the background fluorescence, the average background value was then subtracted from all values in that RTD (Wilson et al. 1986). The dye was pre-mixed into 4 gallons of water taken at the site before input to the creek. The tracer dye used in this study was Rhodamine WT (20% solution, Keyacid) an organic compound that is safe for use in water supply systems and the most widely used tracer for RTD studies (Kilpatrick and Wilson 1989; Wilson et al. 1986).

Spatial sedimentation patterns downstream of the avulsion point were established using an array of sediment-trapping turf mats. Turf mats were installed prior to water year 2010 & 2012 to estimate sedimentation patterns and trapping ability of the northeast floodplain & wetlands respectively.

2.2 Sediment retention on ALBA wetlands

A central goal of this study was to assess the influence of constructed ponds on the sediment retention function of the Triple M Ranch. The ponds of interest were those excavated into the southern and northern wetlands, as they are the ponds with the most interaction with water flowing through the property. Sediment retention on the ranch was estimated four ways. 1) Calibrated stream gages were established upstream of the ranch and at the downstream terminus of the property to calculate a sediment budget. 2) Annual topographic surveys of the northern and southern wetlands were performed to estimate the elevation changes related to deposition or erosion, 3) Turf mat sediment traps were deployed one year to more accurately estimate the sediment retention and to elucidate the subtle sedimentation patterns within the wetlands. 4) Lastly, staff plates were erected in the deepest point of each constructed pond so that sediment trapped by the ponds could be estimated. Methods for these four approaches are detailed below.

2.2.1 Stream gaging and event sampling

Sediment retention on Triple M Ranch was estimated by subtracting the total sediment mass leaving the property from the sediment mass entering the property using stream gages at Johnson Road Bridge and Sill Rd. (Fig 9).

$$\text{Sediment Retention} = \text{Sediment Input} - \text{Sediment Output}$$

Sediment input to Triple M Ranch was estimated by rating a pressure gage located at Johnson Bridge (Fig.9) for water and both suspended and bedload sediment discharge. Suspended sediment concentration samples were taken with a DH-48 depth-integrated sampler at Johnson Bridge and Sill Road and processed at CSUMB in accordance with standard protocols. (CCoWs 2004, Guy 1969). Bedload transport entering the property through Johnson Bridge was measured using a Helley-Smith sampler using standard methods (Guy and Norman 1970, IAEA 2005).

Sediment rating curves were constructed from instantaneous bedload and suspended load measurements regressed against corresponding discharge. Sediment-rating curves were modeled as a power function or second-order

polynomial. For polynomial curves, a linear function was used for discharge less than 26 cfs at Johnson bridge to avoid negative values of suspended load. These rating equations were applied to the continuous gage record of flow, yielding a continuous record of sediment transport. Finally, the instantaneous sediment transport rates were multiplied by the stream gage time interval (15 minutes) to calculate the increment of sediment mass that had passed the gage during each 15 minute time block. The total sediment input was the sum of the incremental sediment masses through the year.

A small ungaged side channel contributed sediment to the northern floodplain (Fig. 9), so sediment input from the channel was estimated. To estimate the sediment input, we assumed that the sediment input was the same as the Johnson Bridge input, diminished by the ratio of watershed areas of the tributary and Johnson Bridge. The proportion was determined to be:

$$Q_{susSide} = 0.058 \times Q_{susJohnson}$$

where $Q_{susSide}$ (g/s) is the suspended sediment discharge entering from the side channel and $Q_{susJohnson}$ (g/s) is the suspended sediment discharge passing by Johnson Bridge. No bedload was seen entering from the side channel, so bedload was assumed to be insignificant.

Sediment output was estimated using the same techniques at the Sill Rd gage, with one exception. The bedload transport was not measured at Sill after the first few storms. All bedload is trapped before reaching Sill Rd. Backwater in the channel upstream of the wetlands causes nearly all bedload (sand and small gravel) to be deposited before flow enters the southern and northern wetlands. No bedload exits the property (Largay 2007).

Continuous gaging was possible in 2010, 2011, 2012, 2014, and 2015, but the approach was hampered by drought conditions and 2013 was ungagged because pervasive algal mats precluded standard stream gaging techniques at Sill Rd.

2.2.2 Topographic surveys

Sediment trapping was also estimated by performing a series of floodplain topographic surveys. Topographic surveys before and after winter runoff of

water year 2010 were performed in the northeast floodplain to document bedload trapping in that area. Floodplain-spanning topographic transects were measured by *Nikon NPR-362* total station on the southern and northern wetlands in 2010, 2013, and 2015 to document any large-scale changes in floodplain elevation (Fig 14).

Detailed topographic surveys of a three of the constructed ponds (ponds 1, 2 and 3; Fig. 12) before and after the storm runoff of water year 2014-15 documented the influence of the constructed ponds on sedimentation rates. The subset of pools were selected for measurement were those closest to the crevasse splay, because they would be most likely to experience sediment trapping. The topographic points were interpolated to make a digital elevation model of the ponds. Raster subtraction of the models provided a quantitative and visual assessment of sediment trapping within the ponds.

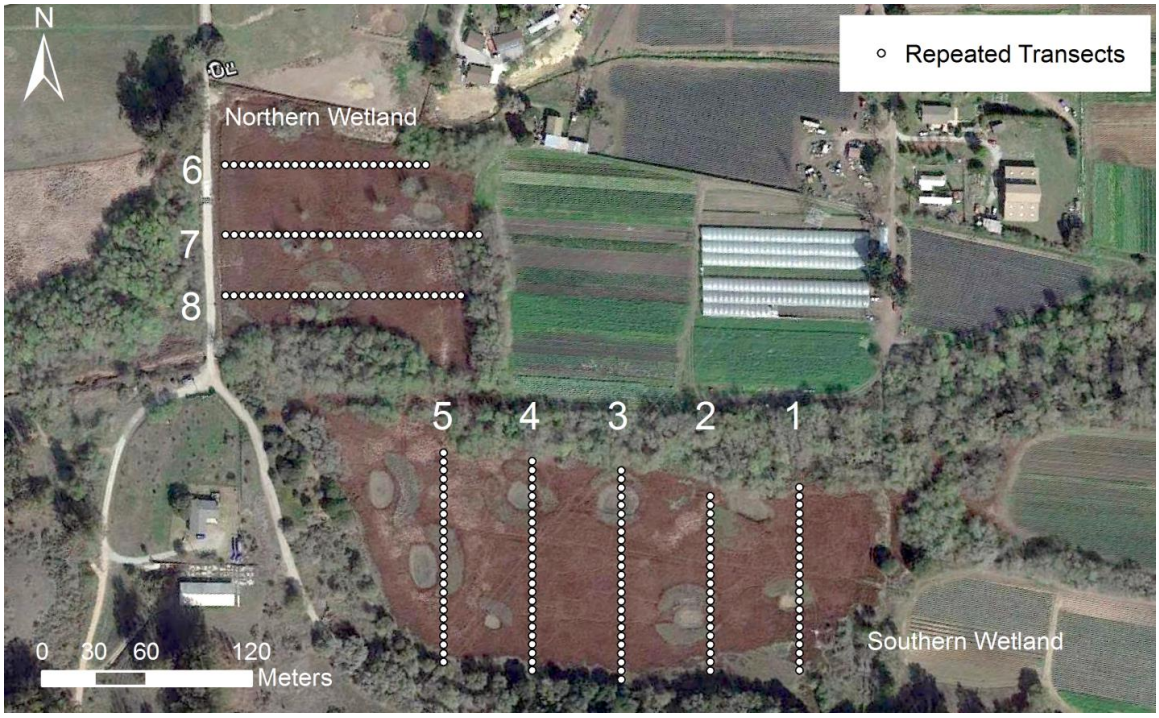

Figure 14: Eight benchmarked topographic survey transects were used to estimate sediment retention through changes in wetland substrate elevation.

2.2.3 Turf mat sediment traps

Field Methods

A pilot study of turf mat sediment trapping was performed in 2010 to assess the sediment-trapping role of the northeast floodplain. A total of 48 turf mats were randomly placed on the Northeast floodplain at the beginning of 2010 water year. They were weighed before and after deployment to estimate the sediment retention. Using the lessons learned from the pilot study, a much more thorough turf mat deployment was used in 2012 to assess the mass and spatial distribution of sediment retained on the southern and northern wetlands.

Fifty seven turf mats were placed in the southern and northern wetlands prior to 2011-12 water year. The goals were to estimate the sediment retention, determine the spatial distribution of sediment, and to assess which environmental variables influenced spatial sedimentation patterns. The following parameters were measured at each sediment trap location: (1) area-normalized sediment deposition (g/m^2), (2) position relative to flow entering the wetland (m), (3) elevation (m), (4) area-normalized vegetation mass (kg/ m^2), and (5) predominant vegetation type. Turf mat position and elevation were measured with a Nikon NPR-362 total station. We distributed the mat locations to cover the wetland extent, and so that each environmental variable in the study was sufficiently replicated (Fig. 15).

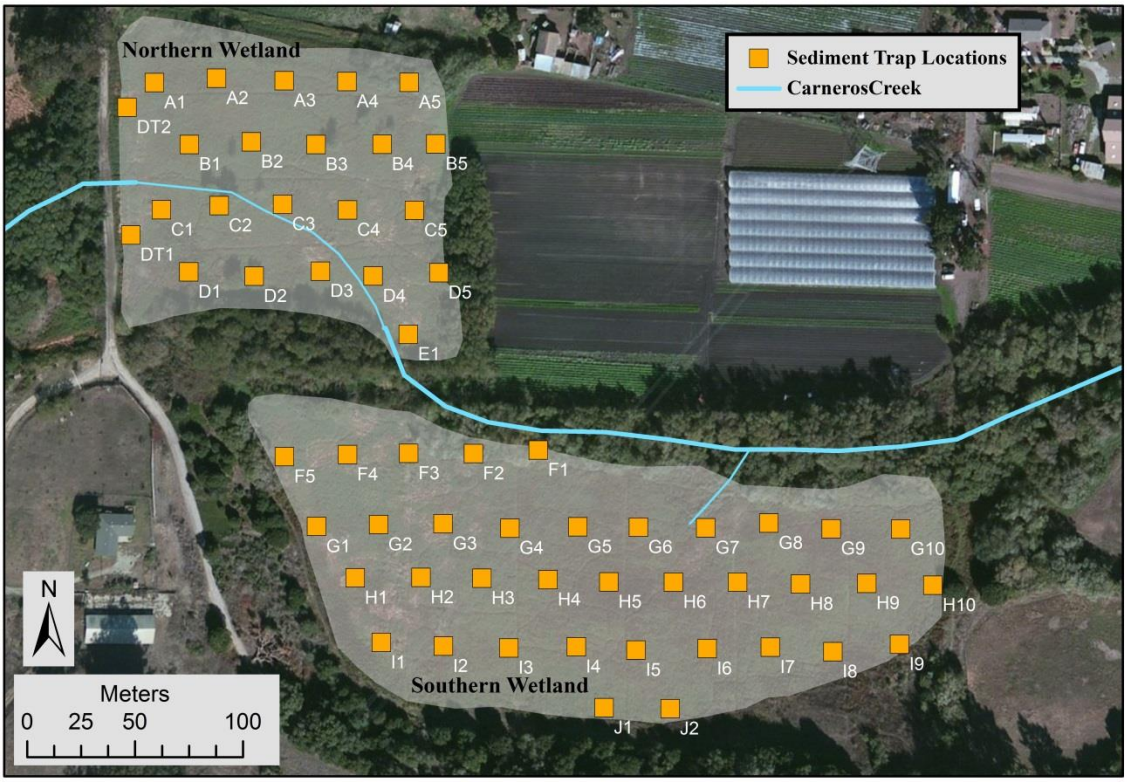

Figure 15. Aerial view of the southern and northern wetlands showing the turf mat sediment trap designations and locations.

All sediment traps were collected at the end of the water year once the ground became sufficiently dry. Any sediment clinging to the bottom of the mat was scraped off in the field before the mat is placed in an individual 13 L bucket.

Laboratory methods & analysis

The dry mass of trapped sediment on the artificial grass mats was determined through methods outlined by Steiger et al (2001). Using that approach, the area-normalized sediment mass retained by each turf mat was calculated as:

$$S_{trap} = S_{gr} + (S_{veg})(veg\ density)$$

where S_{trap} (kg/m^2) is the area-normalized total amount of sediment trapped, S_{gr} (kg/m^2) is the sediment deposited on the upper surface of the mat, and S_{veg} (g sediment/ g plant) is the sediment trapped on the leaves and stalks of the

vegetation. *Veg density* is the measured density of vegetation in the field (kg plant/m^2). It is assumed that the sediment trapped on the artificial grass mats was representative of the sediment trapped on the ground surface throughout the wetland, and therefore provide the S_{gr} value. Early laboratory analysis of S_{veg} indicated that it was far too small to significantly impact the total estimated from the sediment-trapping mats alone. We therefore omit the S_{veg} term from future calculations and modeling.

We extrapolated the turf mat values to the total wetland area through surface modeling. Using the S_{trap} values obtained from the sediment traps, a modeled depositional surface was created by kriging in ArcGIS (Asselman and Middlekoop 1995). Kriging allows the interpolated variance to be estimated and plotted, thus providing some measure of uncertainty. The average value for the interpolated surface was calculated and multiplied by the depositional area, as determined through field surveys, to determine the total mass of sediment deposited over the wetlands.

2.2.4 Pond staff plates

Five-foot tall (≈1.5 m) staff plates were attached to "T-bar" driven into the lowest point of each constructed ponds in the northern and southern wetlands before the 2014-15 winter runoff (Fig. 12). Each staff plate was installed with the 0 m stage flush to the soil surface. The thickness of sediment retained in pond bottom was directly read from the staff plate.

2.3 Assessing future sediment retention

We assessed how wetland sediment trapping might be influenced by both climate change and urban expansion in the watershed. The results of the climate response are from the literature, whereas the results of urbanization are from hydrologic modeling and literature reviews. We used the Army Corps of Engineers Hydrologic Engineering Center Modeling System (HEC-HMS) to create a hydrologic simulation model for the Carneros watershed (Fig. 16). Components of the model include: a basin model, a meteorologic model, a control specification and time-series precipitation.

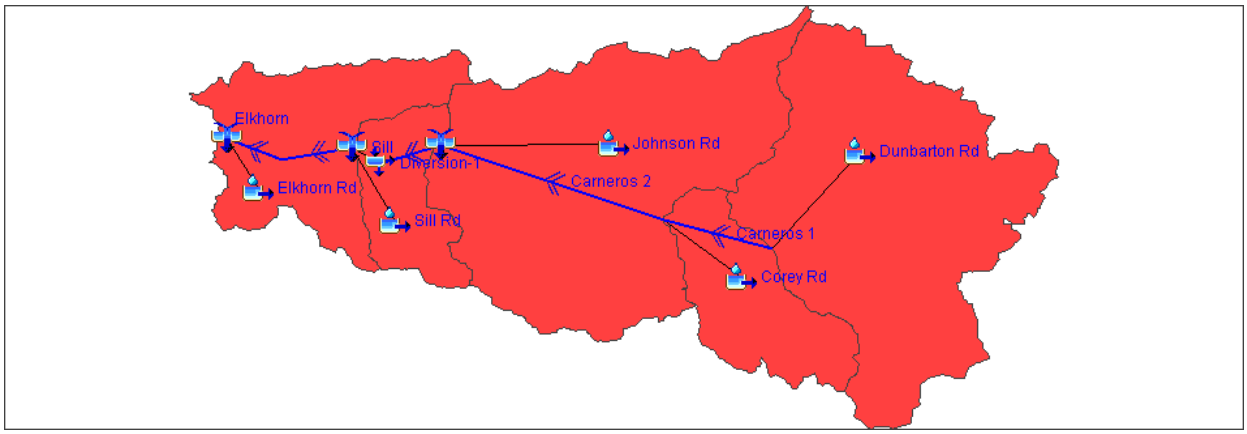

Figure 16. HEC-HMS model layout of the Carneros watershed showing sub basins.

Within the basin model, parameters including canopy storage, surface storage, base flow, and groundwater storage were accounted for in five sub-basin components. The sub-basins were connected by five reaches. The reach elements represented stream processes such as stream routing, channel roughness, and percolation. The model output is a synthetic hydrograph at Johnson Bridge, upstream from the Triple M Ranch, based upon precipitation events that are input to the program. We adjusted the model watershed parameters until a reasonable fit was achieved between the synthetic and actual hydrographs for Johnson Bridge gage.

With the loosely calibrated model, we synthesized the hydrograph again using assumed future watershed conditions representing urbanization. The altered hydrographs were interpreted in the context of wetland function based upon a literature review of wetland dynamics. We altered the calibrated HEC HMS model to assess the impact of increased urban development by increasing the % impervious cover in each sub-basin of the watershed, without changing other model parameters.

2.4 Preliminary Channel Design

Natural channel design principles were used to produce an appropriately scaled conceptual design for a channel and floodplain system that could be constructed in place of the northern and southern wetland parcels. This design could be refined and implemented in the event that future resource managers would prefer sediment transport over sediment retention on the Triple M Ranch. The overarching goal in natural channel design is to construct a channel and floodplain system that has two characteristics. The channel should just transport the sediment supplied to it without net aggradation or degradation as measured over many hydrologic cycles (list the main geomorphologists). And, the channel should be sized to flood frequently to sustain the ambient wetland ecosystem. These end goals are approached by emulating natural systems that have those characteristics (Leopold, 1994).

2.4.1 Dimension, Pattern, profile

The channel cross sectional geometry (area (Abkf), width (Wbkf), depth (dbkf), and wetted perimeter (WP)) was obtained from an existing reach of Carneros Creek that has approximately the same drainage area as the restoration site, floods at least annually, and shows no signs of excess erosion or aggradation in the context of transporting the ambient sediment load of Carneros Creek. Hydraulic radius (R) was calculated as

$R = Abkf/WP.$

The cross sectional width was used to scale planform geometry. Meander length (Lm) was calculated using a dimensionless ratio of

$Lm/Wbkf = 11$ (Leopold and Wolman 1960).

Radius of curvature (Rc) was similarly calculated using a conservative ratio of $Rc/Wbkf = 2.7$ (Smith et al. 2009).

Channel slope (Sc) was calculated from the existing valley slope (Sv) and design sinuosity (K) as

$Sc = Sv/k.$

Sediment transport competency was assessed by comparing the average boundary shear stress required to initiate movement of the 84th percentile (d_{84}) of the grain size distribution with the shear stress generated by the design channel. The required shear stress is called the "critical shear stress" (τ_c).

$\tau_c = (\tau^*) \times d_{84} \times (\gamma s - \gamma w)$,

where τ^*, the dimensionless shear stress is calculated from Andrews (1994) as

$\tau^* = 0.0384 \times (d_{84} / d_{50})^{0.887}$

where d_{50} is the median grain size in the bed, γs is the weight density of sediment (29988 N/m^3) and γw is the weight density of water (9807 N/m^3). The average boundary shear stress generated by the design channel (τ_o) was calculated as

$\tau_o = \gamma w \times R \times Sc$.

Finally, τ_o and τ_c were compared to determine if the design parameters were sufficient to transport the d_{84} and to qualitatively assess whether the difference ($\tau_o - \tau_c$) left enough excess shear stress to transport the moderately large volume of sand sourced in the watershed.

2.4.2 Hydraulic Modeling and Sediment Transport

The stream design hydraulics were modeled using Army Corps of Engineers Hydrologic Engineering Center River Analysis System (HEC-RAS). The input of the model included vertically-referenced, synthetic cross sections derived from the stream design, and estimated channel roughness coefficients. The model was run to determine bankfull discharge, which could then be assessed for frequency through partial duration analysis of stream flow records. The model output also includes another estimate of τ_o for comparison with the estimate described in the previous section.

3 Results

3.1 ALBA wetland flow dynamics.

Two studies were completed to assess wetland behavior, and to analyze the processes that lead to sedimentation in an unmanaged wetland. The first study utilized dye tests to analyze retention time and its controls (Holloway 2010). The second study used turf mat sediment traps in the 2012 water year to determine both the total sediment retained on the floodplain and to analyze the spatial patterns of sediment retention (Bassett, in review). This section summarizes the results of Holloway (2010) and the spatial distribution of sediment retention portion of Bassett (in review). The text below largely verbatim from the two cited theses, whose authors are also coauthors on this report.

3.1.1 Residence time.

The residence time, or time to centroid of the residence time distribution varied inversely with stage and discharge (Table 2, Fig. 17), and the residence time distributions were bimodal for all dye experiments from Railcar Bridge to Sill Road (Fig. 17). Average and maximum stage and discharge varied little during three of those four experiments (Table 3). During the slug dye experiment at 0.1 m^3/s average Sill Road discharge, interference and dropout occurred with the fluorometer readings, likely due to an observed oil slick (Fig. 17). For calculations of centroid and other parameters on that experiment, the line was simply connected across the abnormal section. The experiment on 1/29/2010 from Johnson Bridge to Railcar Bridge, at an average Sill Road stage and discharge of 21.4 cm and 0.213 m^3/s, showed little mixing and standard plug-flow. Time to centroid, start, peak, and end was 177, 132, 165, and 251 minutes, respectively (Fig. 18). The experiment on 2/6/2010 from Johnson Bridge to Sill Road used too little dye to register on the fluorometer.

Table 1. Residence time distribution parameters for the four slug dye experiments from Railcar Bridge to Sill Road in hours and minutes.

Sill Road Avg. Discharge (m^3s^{-1})	Start	Peak 1	Centroid (Residence Time)	Peak 2	End	Fluorometer Record Ends
0.001	5:48	7:49	27:50	30:16	41:32	119:27
0.1	13:00	17:03	19:42	25:37	28:46	89:35
0.26	1:41	2:11	12:23	9:08	30:11	91:31
1.24	1:19	1:58	2:51	57:01	58:27	73:39

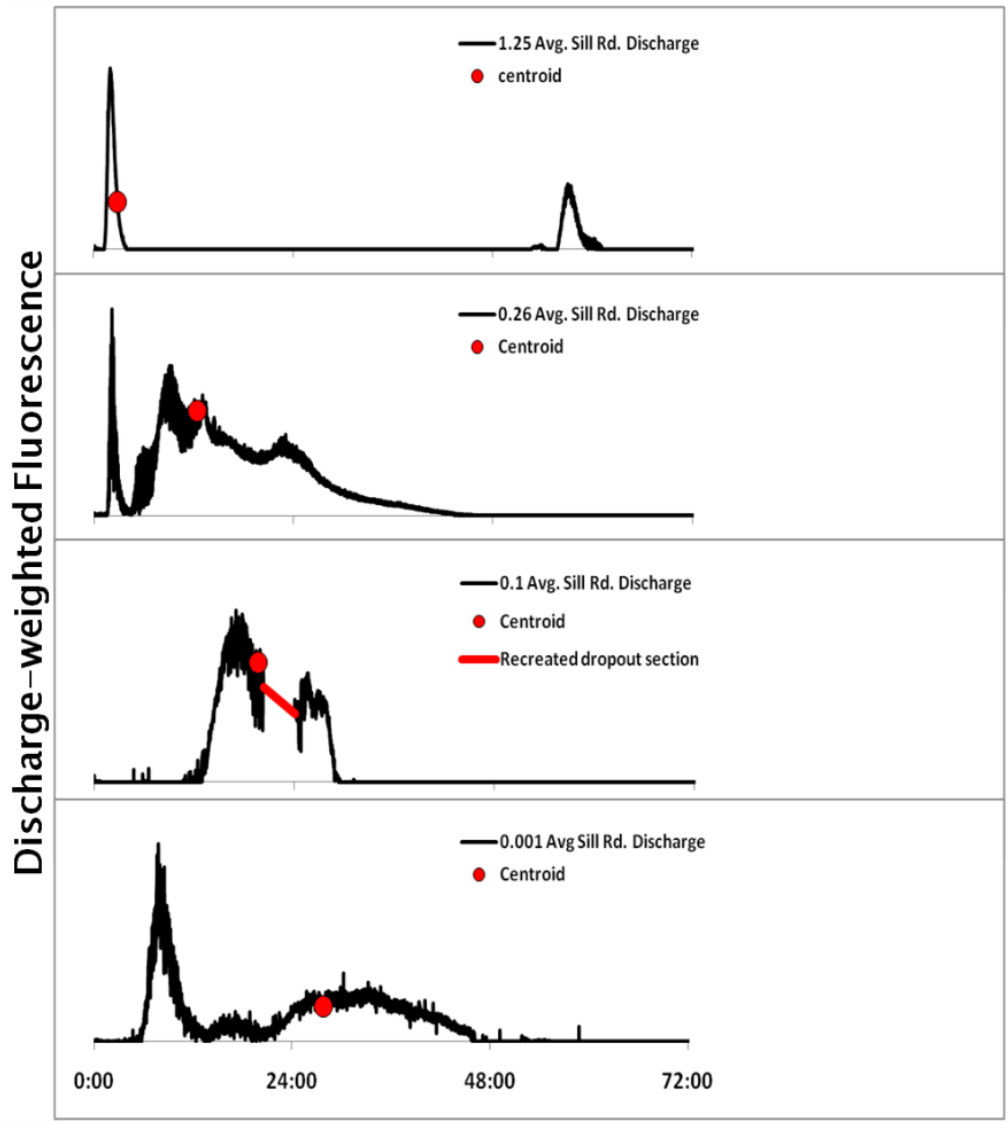

Figure 17. Residence time distributions from Railcar Bridge to Sill Road labeled by average stage at Sill Road during experiment. Time in hours to centroid (red circles) varies inversely with discharge.

Table 2. Maximum and average stage and maximum discharge during four slug dye experiments from Railcar Bridge to Sill Road.

Sill Road Avg. Discharge (m^3s^{-1})	Sill Road Max. Stage (cm)	Sill Road Avg. Stage (cm)	Sill Road Max. Discharge (m^3s^{-1})
0.001	6.4	5.4	0.001
0.1	19.8	19	0.130
0.26	26.8	22.9	0.406
1.24	51.4	33.4	5.179

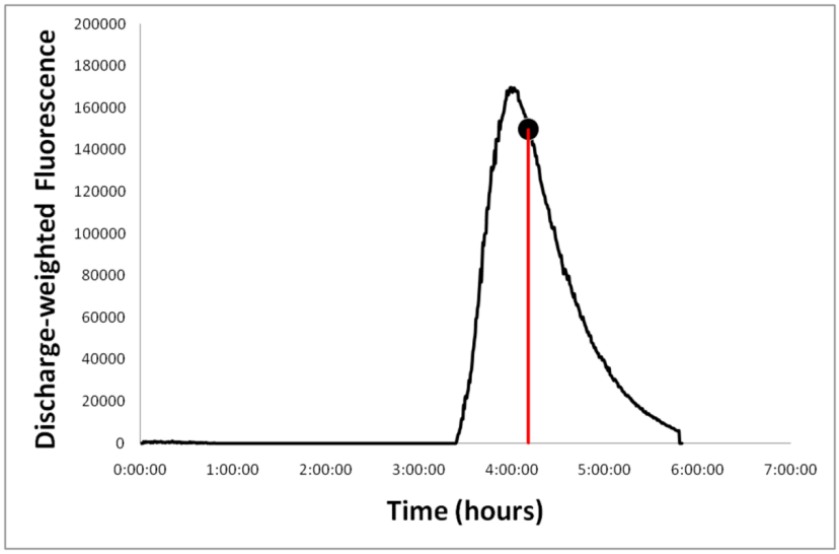

Figure 18. Residence time distribution from Johnson Bridge to Railcar Bridge during an average stage of 0.18 m³/s at Sill Road.

3.1.1.1 Prediction of times to centroid

The time to centroid as a function of stage from Railcar Bridge to Sill Road showed longer residence times occurred at lower stages (Fig. 19).

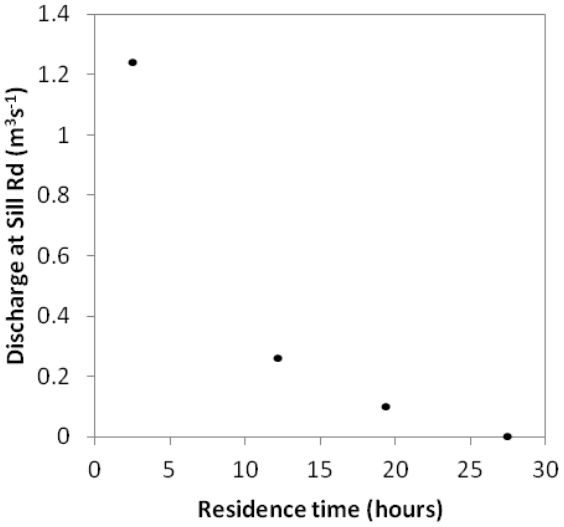

Figure 19. Relationship between time to centroid and discharge at Sill Road during dye experiments from Railcar Bridge to Sill Road.

3.1.2 Sedimentation patterns.

Water year 2012 produced below average rainfall throughout the region. There was 39.8 cm precipitation recorded on site (Fig. 20), which is below the median of 53 cm/yr as historically measured at a site located 7 km to the northwest (Largay 2007). Stream flow initiated at the upstream gaging location on 5 Oct 2011, and ceased for the season on 1 May 2012. However, the creek remained completely dry for a substantial portion of the water year in October through mid-January as well (Fig. 20). Five major flow events were measured by the study pressure transducers, with runoff volume totaling 8.36×10^5 m^3. The seasonal peak flow was approximately 2.3 m^3 /s. In contrast, the downstream gaging location measured a total of 5.37×10^5 m^3 over four major flow events that began 21 January 2012 and ceased 27 April 2012, with a peak of 2.5 m^3 /s. Losses between the gages resulted from some combination of evapotranspiration, infiltration to groundwater, and slow leakage through the sand occluding the canal downstream of the study site.

Figure 21 shows the sediment data and rating curves used to calculate the sediment transport calculations presented in Table 4.

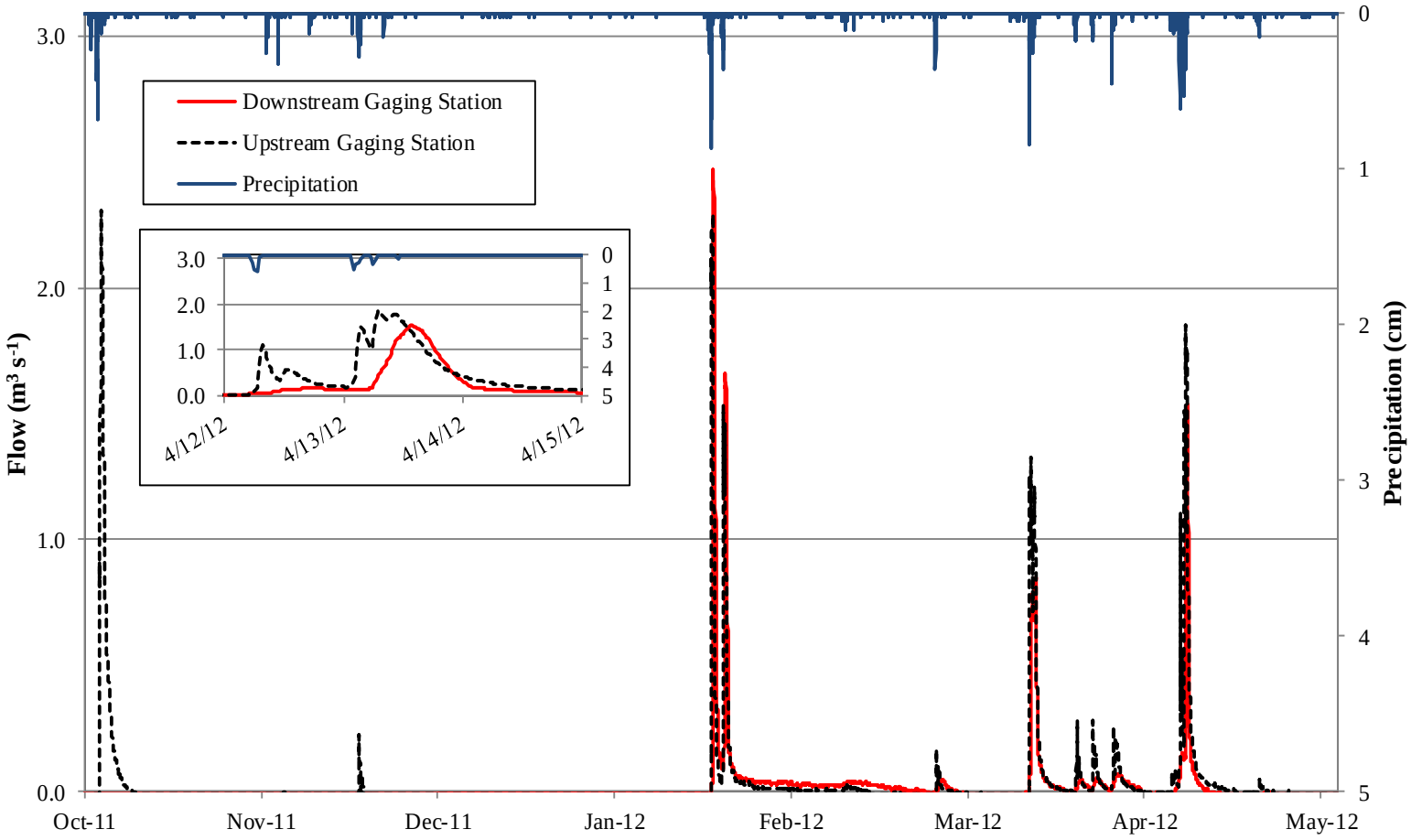

Figure 20. The plotted hydrographs for the upstream and downstream gages. Precipitation is shown inverted on the secondary axis. Note the downstream gage did not receive runoff from the first storm due to the volume of the wetlands. An April storm event is highlighted in the inset box, illustrating the lag between peaks and the lack of downstream flow as the wetland basin becomes inundated.

Table 4. Summary of suspended sediment, bedload sediment, and flow entering and exiting the study location.

Flow – Upstream (IN)	8.36×10^5	m^3
Flow – Side tribs (IN)	4.85×10^4	m^3
Flow – Downstream (OUT)	5.37×10^5	m^3
Flow – difference	3.48×10^5	m^3
Suspended Sediment – Upstream (IN)	1.91×10^5	kg
Suspended Sediment – Side tribs (IN)	1.11×10^4	kg
Suspended Sediment – Downstream (OUT)	3.51×10^4	kg
Suspended Sediment – difference	1.67×10^5	kg
Bedload Sediment – Upstream (IN)	1.41×10^4	kg
Bedload Sediment – Downstream (OUT)	0	kg
Bedload Sediment – difference	1.41×10^4	kg
Total Sediment Trapped	1.81×10^5	kg

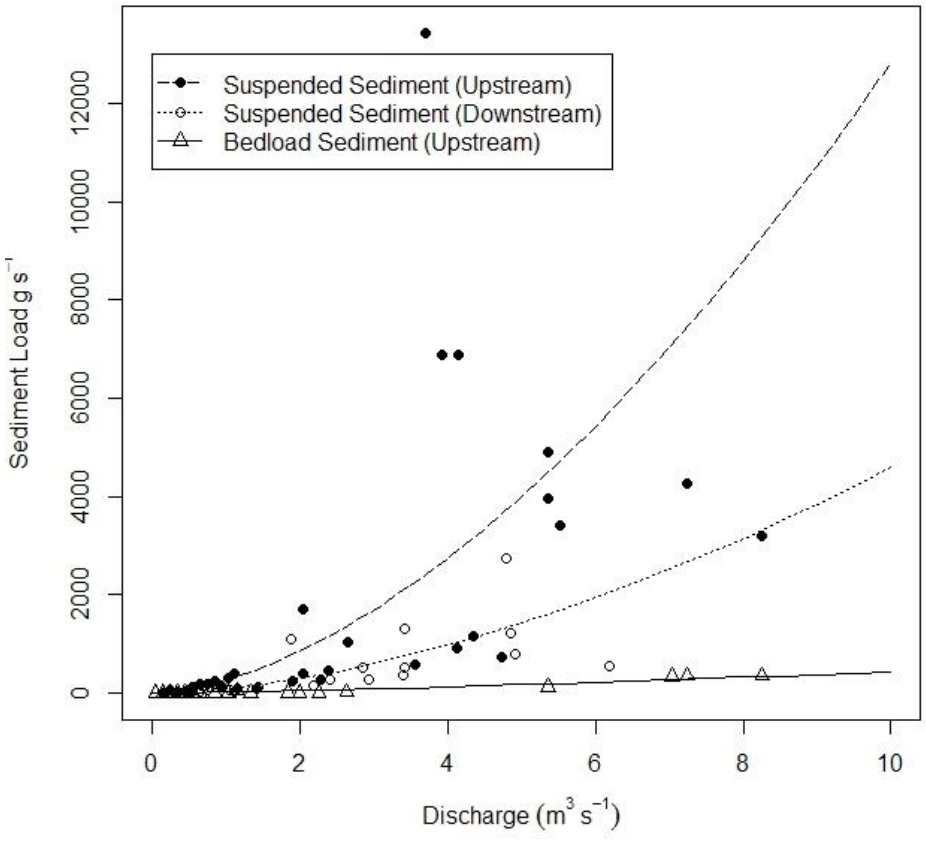

Figure 21. The suspended and bedload rating curves and plotted data for both gaging locations.

3.1.3 Sediment Traps

Of the 59 sediment traps installed, 56 were recovered and cleaned of sediment for analysis. Three of these collected mats were located slightly above the level of inundation reached during the study, and were excluded from further analysis. Trapped sediment ranged from 22.9 g to 258.8 g, with an average of 94.9 g, equating to an area density of 254.0, 2875.2, and 1054.6 g/m^2, respectively (Fig. 22). The mass of the trapped organic component ranged from 3.0 g to 32.4 g, with a mean of 13.2 g. On average, the sediment traps collected 87% sediment and 13% organics by mass.

As determined through GIS surface interpolation (Fig. 23), the southern wetland retained a total of 3.5×10^4 kg (35 tonnes) of sediment, with an average, minimum, and maximum of 1050, 230, and 1812 g/m^2, respectively. The northern wetland retained a total of 1.7×10^4 kg (17 tonnes) of sediment, with an average, minimum, and maximum of 851, 332, and 2875 g/m^2, respectively. Both wetlands combined trapped 5.2×10^4 kg (52 tonnes) of sediment, as determined through the interpolation of the sediment trap data (Figure 23). Vegetation density ranged from 0.19 to 7.09 kg/m^2, and averaged 3.35 kg/m^2 (Fig. 24). Mat elevation ranged from 1.378 – 2.828 m, with an average elevation of 2.373 m (Fig. 25). The sediment traps ranged from 18.4 – 193.1 meters from the point of inflow (Fig. 26).

A series of general linear models were used to determine the relative influence of environmental factors on the response variable—area-normalized sediment deposition (g /m^2). Each of the modeled input variables was described as a continuous positive value with a gamma error distribution, with the exception of vegetation type, which is categorical. The model utilized the four predictor variables described here. (1) "Distance (m) from point of inflow" was defined as the map distance between the sample plot and the nearest point on the delineated inflow polygon as measured using ArcGIS. (2) "Relative average water depth (m)" was indexed as the elevation of the plot. (3) "Vegetation density (kg/m^2)" was calculated as the area-normalized dry mass of vegetation stalks and leaves located near the plot. (4) "Vegetation type" assessed the influence of the physical differences of the two dominant vegetation types: smartweed (*Polygonum amphibium*) and reed (*Typha spp.*). The models were constructed using the R statistical package (R Development Core Team, 2010) using the following general linear model:

$$Y = \beta_0 + \beta_1 X_1 + \cdots + \beta_n X_n$$

where β_0 is the model intercept, $\beta_i \ldots \beta_n$ are the parameter coefficients corresponding to predictor variables $X_1 \ldots X_n$. See Bassett (in review) for statistical details of the model.

The twelve models (Table 5) were compared using Akaike's Information Criterion (AIC), which ranks the predictive strength of each model relative to the others. AIC was used to determine which combination of parameters created the model that best replicates sediment deposition (Burnham and Anderson 2002). Instead of examining all possible models, eleven models (plus the null model) were selected a priori based on field observations and findings from previous sedimentation studies.

Table 5. The twelve models included in this study. DIST refers to the Cartesian distance from the point of inflow, ELEV refers to the elevation of the sediment trap, VEG_Mass refers to the mass of vegetation at the trap location, and VEG_Type refers to the type of vegetation at trap location (*Polygonum* or *Typha*). K corresponds to the number of parameters in each model.

Model	Parameters Included	K
M0	Null (sediment is not influenced by modeled factors)	1
M1	DIST	1
M2	ELEV	1
M3	VEG_Mass	1
M4	VEG_Type	1
M5	VEG_Mass + VEG_Type	2
M6	ELEV + VEG_Mass	2
M7	DIST + ELEV	2
M8	DIST + VEG_Mass	2
M9	DIST + VEG_Mass + VEG_Type	3
M10	DIST + ELEV + VEG_Mass	3
M11	DIST + ELEV + VEG_Mass + VEG_Type	4

The model incorporating distance from inflow, and vegetation mass (M8) performed the best in the AIC comparison, with M9 (distance, vegetation mass, and vegetation type) and M1 (distance) performing almost as well. The influence of distance from point of entry can be seen in the high rates of deposition at the crevasse splay entering the southern wetland and the small sediment fan at the entry to the northern wetland (Fig. 23).

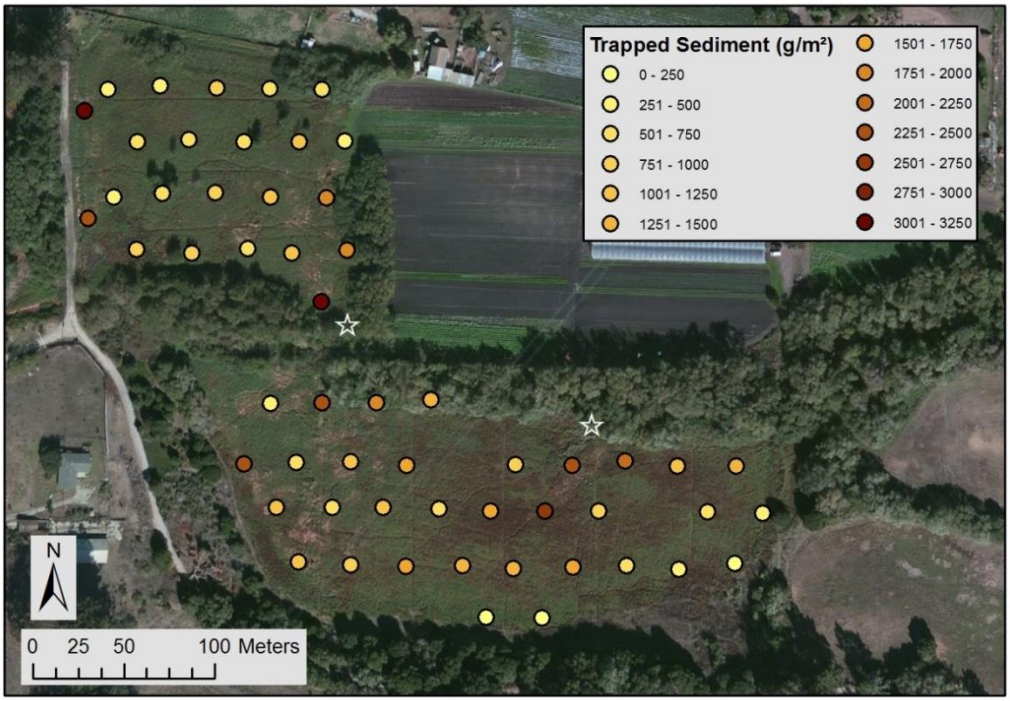

Figure 22. The mass of trapped sediment, in grams per square meter, at each of the recovered sample plots. The points of inflow are marked with a white star.

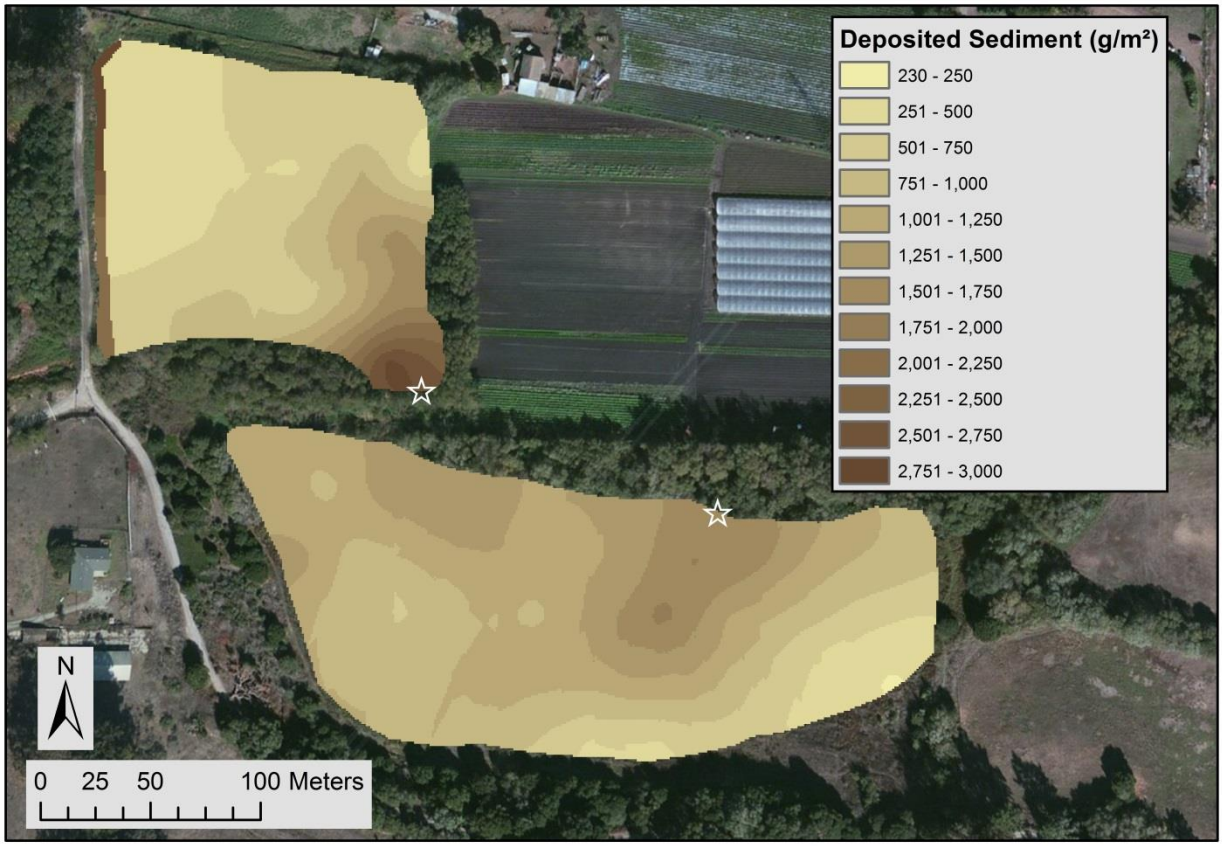

Figure 23. The interpolated surface generated through krigging the sediment traps. Each point of inflow are marked with a white star.

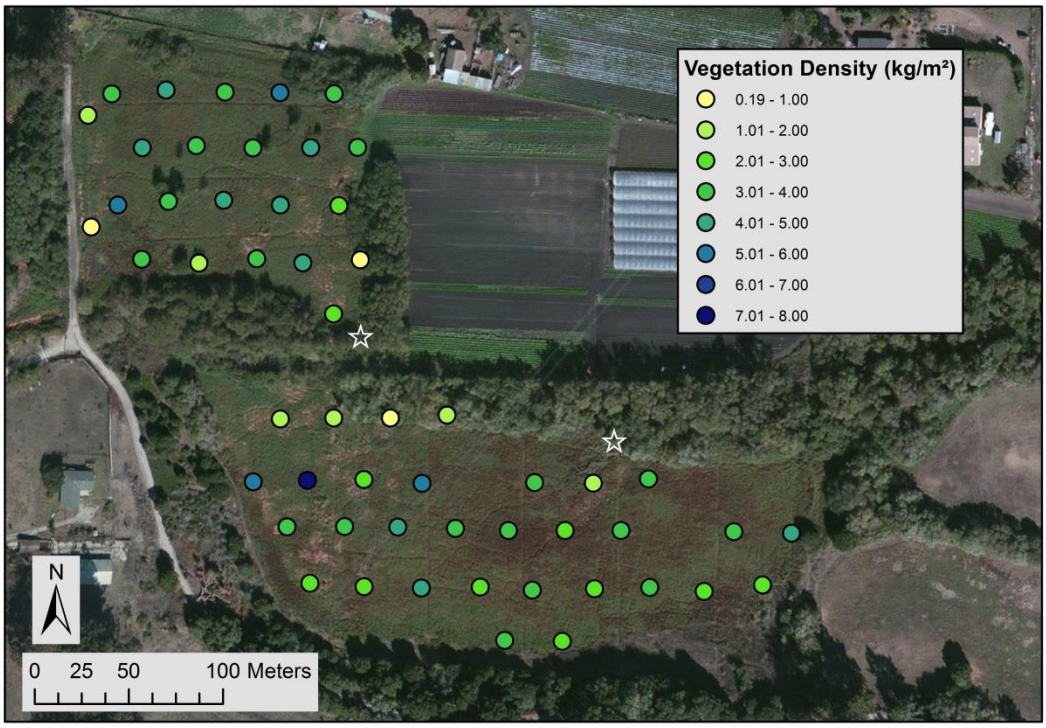

Figure 24. The vegetation density at each of the recovered plots. The points of inflow are marked with a white star.

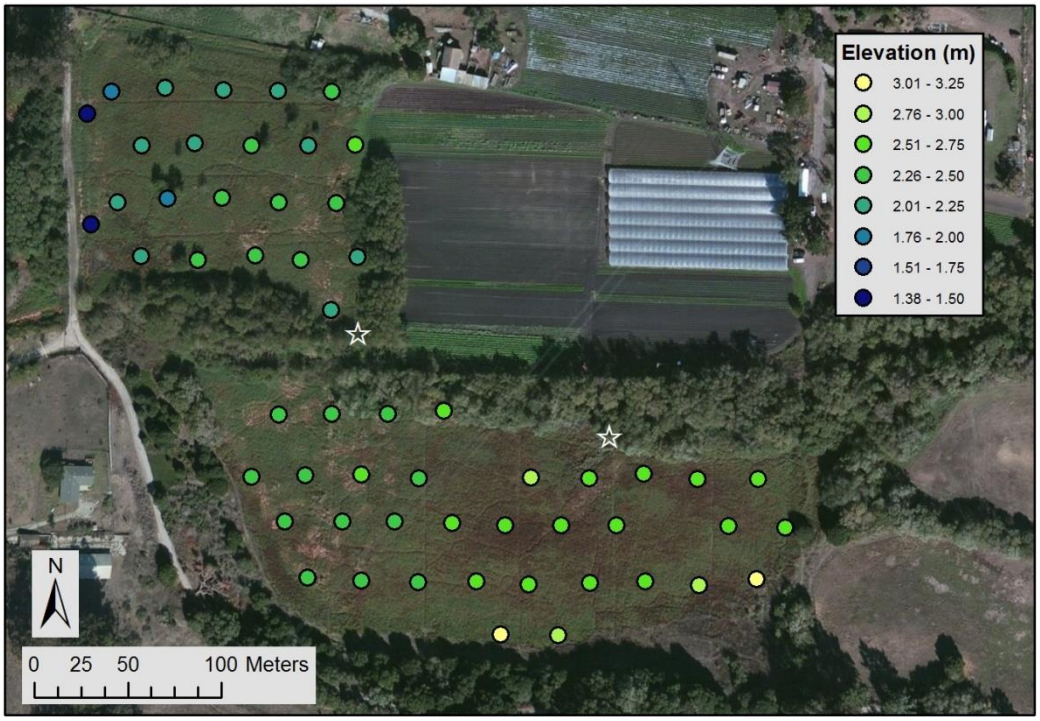

Figure 25. The elevation of each of the recovered sediment traps. The points of inflow are marked with a white star.

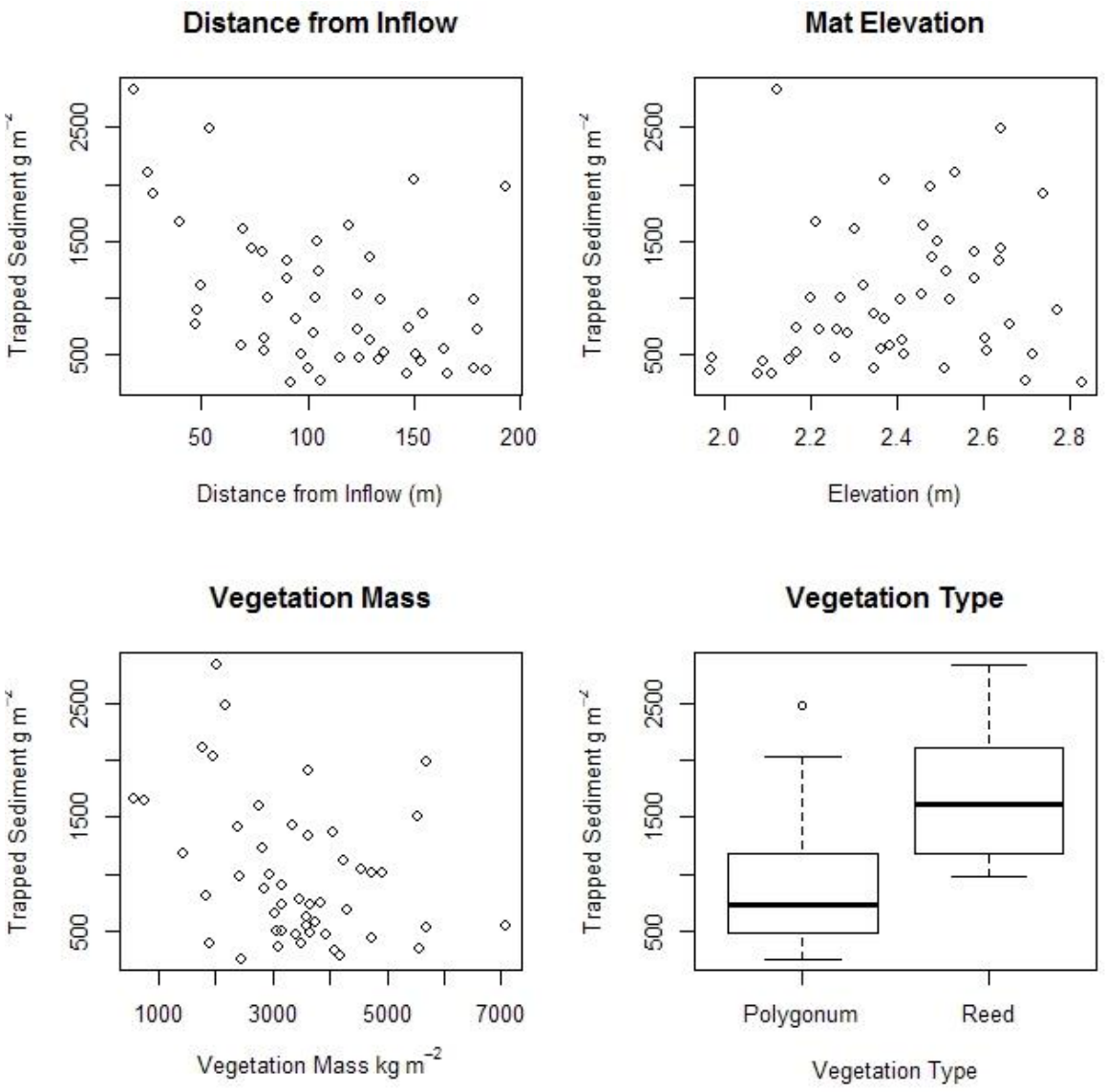

Figure 26. Plots displaying the distance from the point of inflow, sediment trap elevation, vegetation mass, and a box plot of the predominant type of vegetation at each sample location.

3.2 Sediment trapping before and after ponds.

3.2.1 Stream gaging

Carneros Creek was gaged upstream and downstream of the wetlands for water years 2010 to 2015, excluding 2013 (Fig. 27). Water year 2013 was missed because of a pervasive algal bloom that precluded making accurate discharge measurements at Sill Road. It was also the water year immediately after pond and culvert construction.

During the gaged years, the stream gages were rated for sediment discharge as a function of water discharge, and sediment retention was calculated (Table 6). During that time, all bedload was retained on the property, generally upstream of the avulsion point. In 2010 the bedload retention was found to be just 1% of the total sediment retained on the property (Holloway 2010), and no further measurements were made.

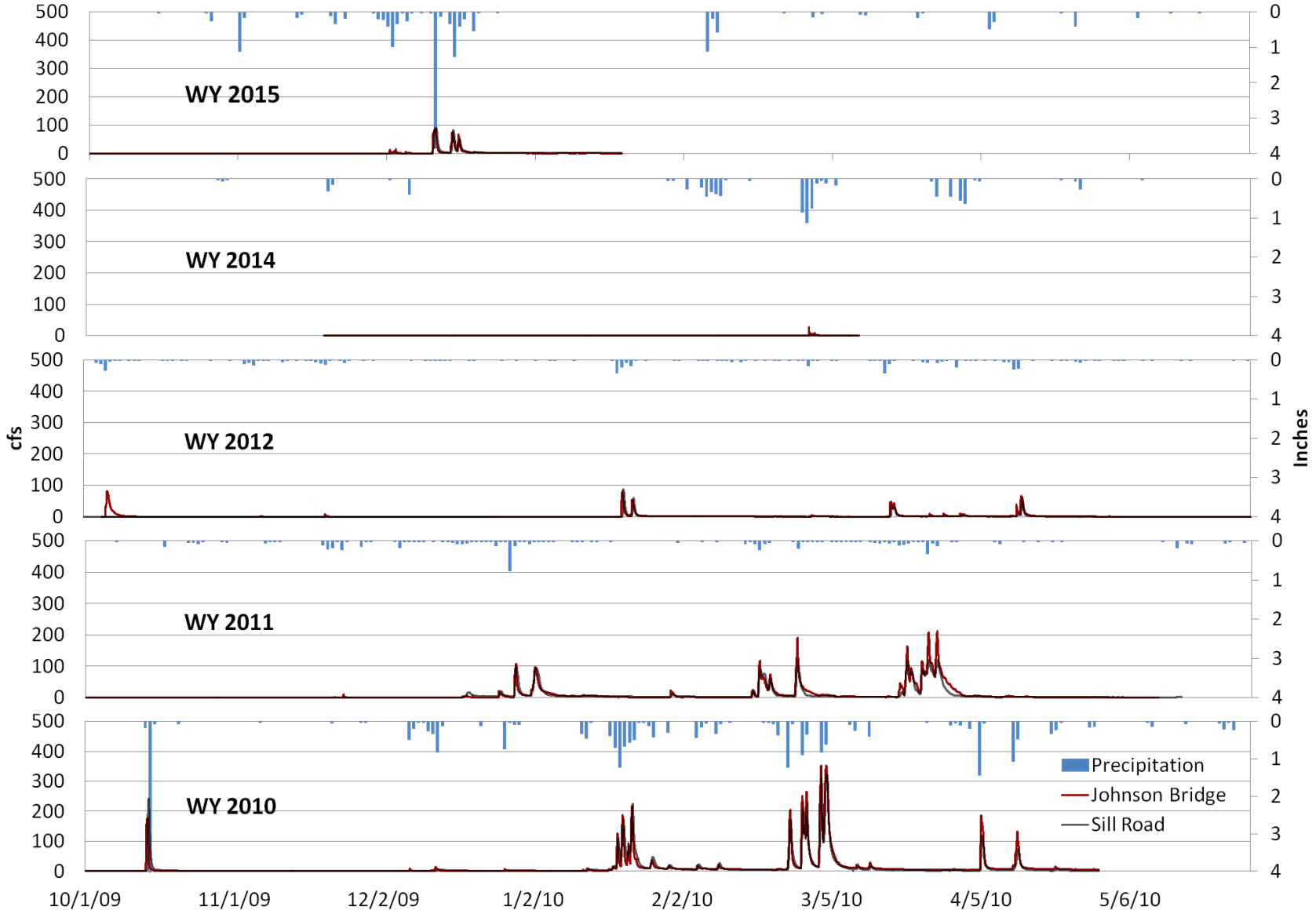

Figure 27: Hydrographs from stream gages located at Johnson Bridge (red) and Sill Rd. (black) plotted with precipitation records (blue).

Table 6: Estimates of wetland sediment retention based upon suspended sediment measurements at stream gages. "In" is suspended sediment mass (tonnes) measured at Johnson Bridge. "Out" is suspended sediment mass (tonnes) measured at Sill Road. "Difference" is the mass (tonnes) of suspended sediment retained.

Water Year	2010	2011	2012	2013	2014	2015
In	3757	2,114	230		22	1,882
Out	1,146	1,032	38		10	287
Difference	2,611	1,082	192		12	1595
% Retained	68	46	82		55	84

Did sediment retention change following pond construction? Pond construction occurred in 2013, so water years 2014 and 2015 are the "post-pond construction" years in the analysis. The post-construction years were the continuation of several drought years (Fig. 27). It is important to compare water years with similar runoff characteristics because there is a strong relationship between discharge and residence time (Fig.19), which is a key factor in sediment retention.

There are no pre-construction years comparable to the very dry post-construction 2014 water year. The hydrograph of post construction year 2015 is reasonably comparable to pre-construction year 2012, so we can compare those years for sediment retention. Although the magnitude of sediment entering and leaving the wetlands is considerably different between those years, the percent of sediment retained was very similar. The difference between the before-pond and after-pond values is indistinguishable, given the large uncertainties inherent in such measurements.

3.2.2 Wetland transects surveys

Eight wetland-spanning topographic transects were surveyed for several years to detect changes do to sedimentation (Fig. 14). No patterns of aggradation or degradation were seen between the 2010, 2013 & 2015 surveys (Fig. 28). While deposition certainly occurred (Table 6), the vertical change in topography was too small to capture using standard land survey instruments. Large scale changes present after 2013 were the result of pond construction, not wetland sediment dynamics.

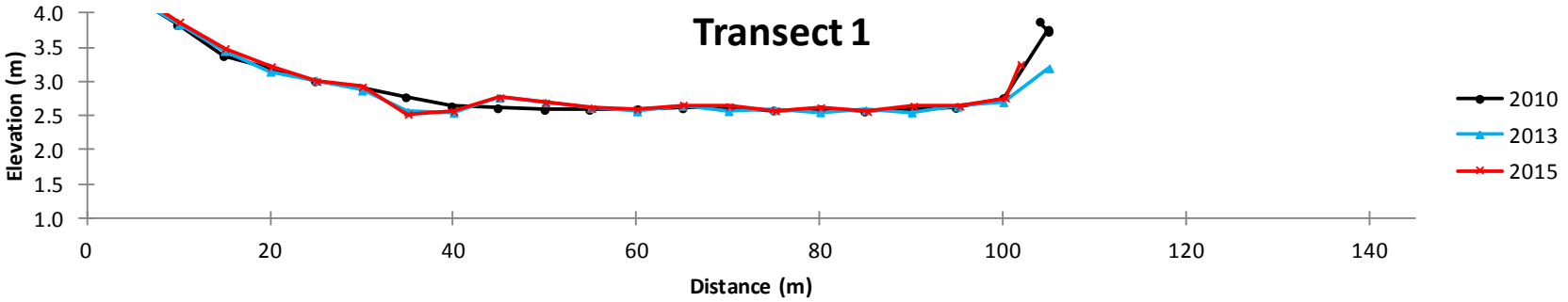
Transect 1
Elevation (m)
4.0
3.5
3.0
2.5
2.0
1.5
1.0
0
20
40
60
80
100
120
140
Distance (m)
2010
2013
2015

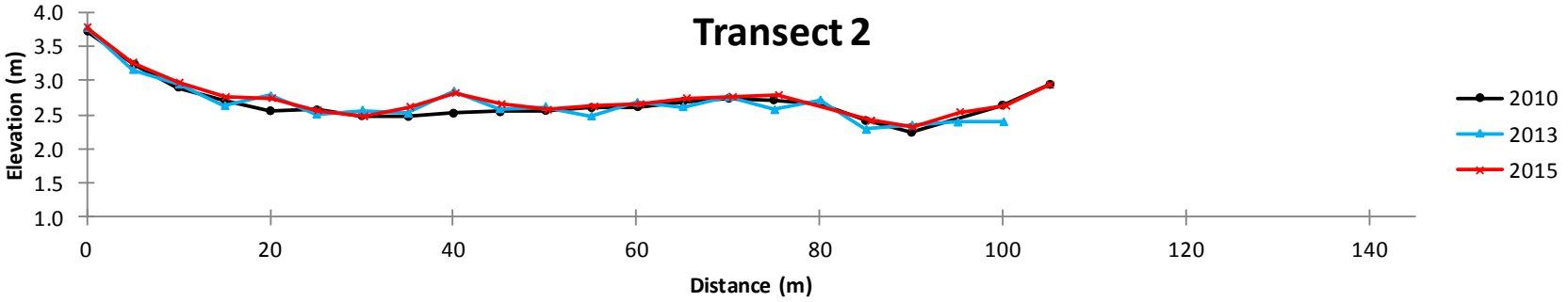
Transect 2
Elevation (m)
4.0
3.5
3.0
2.5
2.0
1.5
1.0
0
20
40
60
80
100
120
140
Distance (m)
2010
2013
2015

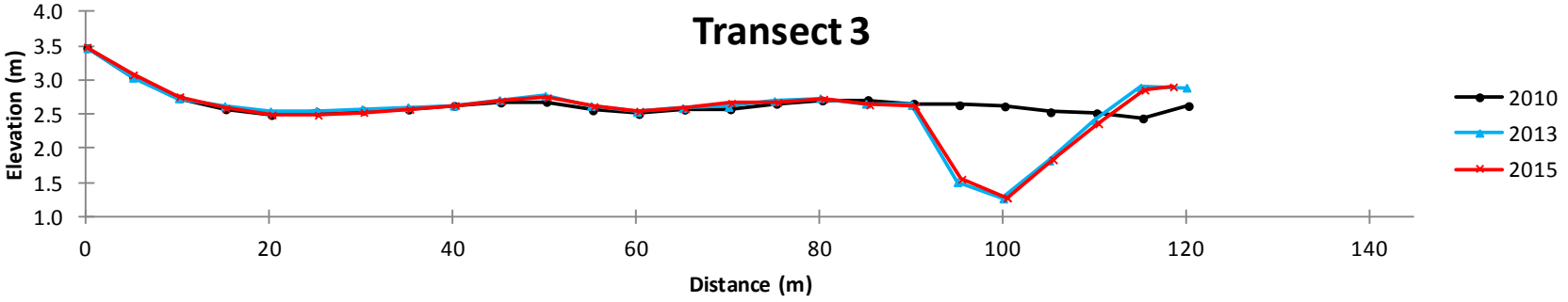
Transect 3
Elevation (m)
4.0
3.5
3.0
2.5
2.0
1.5
1.0
0
20
40
60
80
100
120
140
Distance (m)
2010
2013
2015

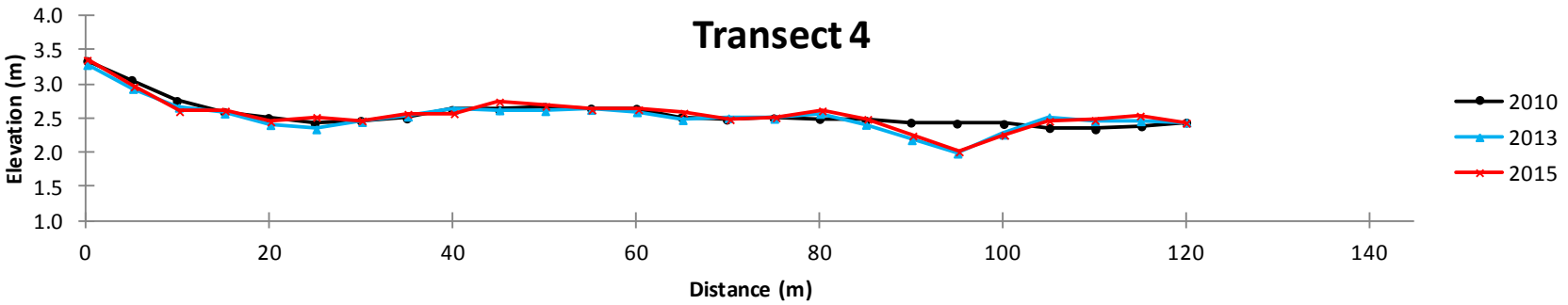
Transect 4
Elevation (m)
4.0
3.5
3.0
2.5
2.0
1.5
1.0
0
20
40
60
80
100
120
140
Distance (m)
2010
2013
2015

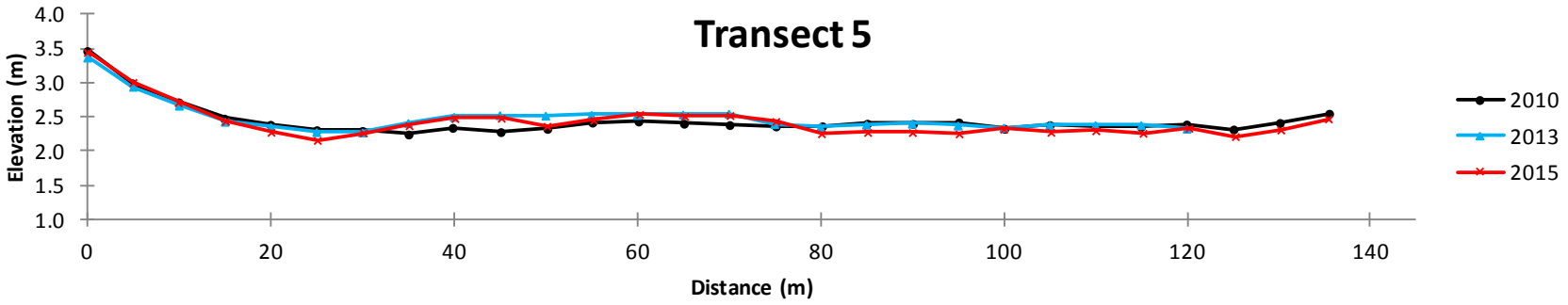
Transect 5
Elevation (m)
4.0
3.5
3.0
2.5
2.0
1.5
1.0
0
20
40
60
80
100
120
140
Distance (m)
2010
2013
2015

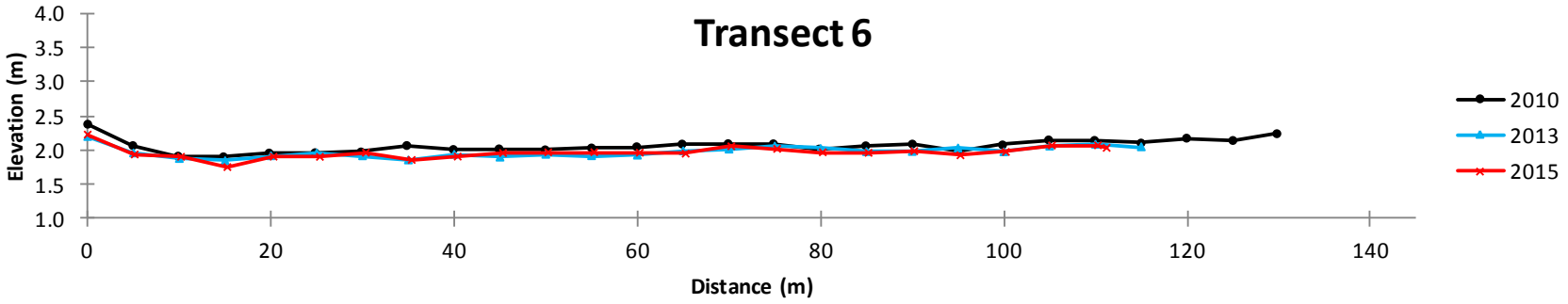
Transect 6
Elevation (m)
4.0
3.5
3.0
2.5
2.0
1.5
1.0
0
20
40
60
80
100
120
140
Distance (m)
2010
2013
2015

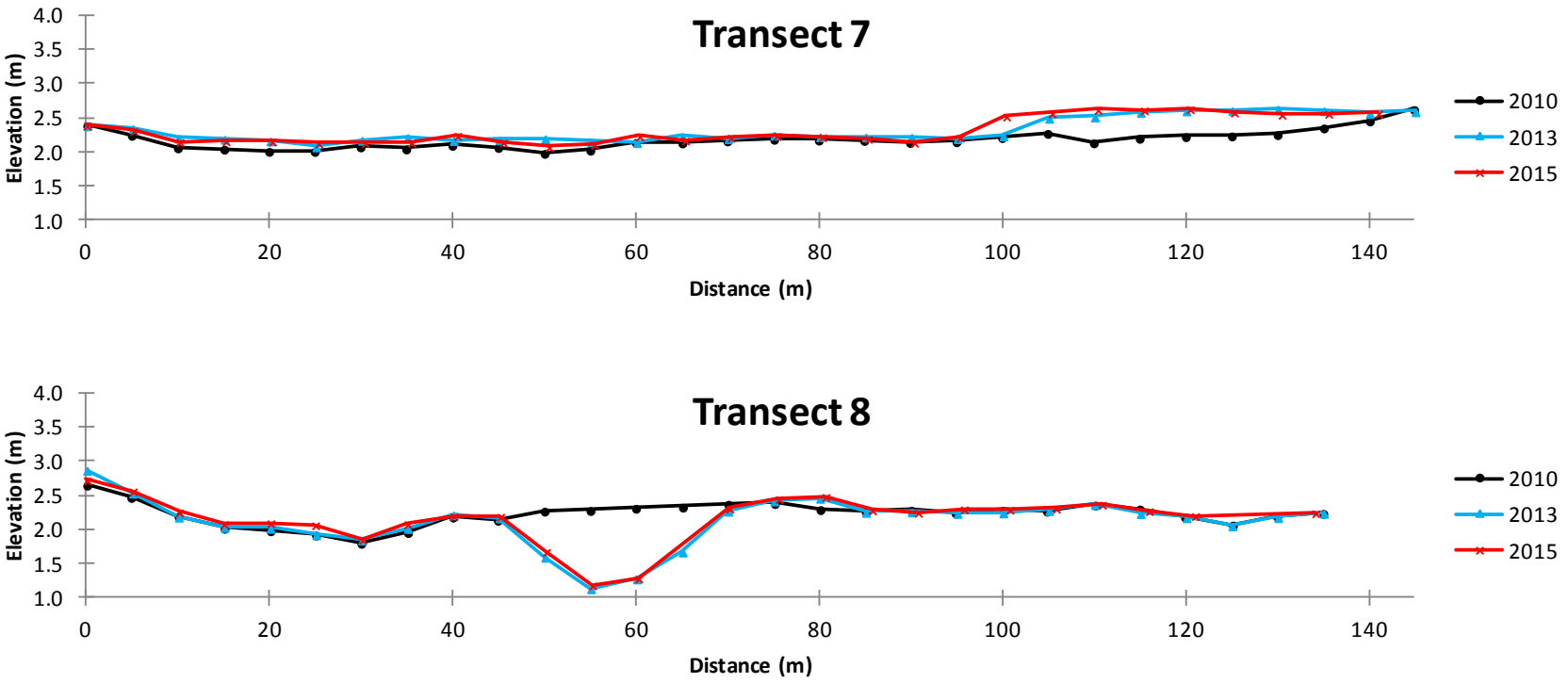

Figure 28: Topographic transects across the wetlands. See Figure 14 for transect locations.

3.2.3 Pond topographic surveys

In the last year of study we looked closely at the ponds in two ways for evidence of sediment trapping, in excess of the surrounding wetlands. First we used raster subtraction of topographic data collected before and after runoff, and second, we assessed how far staff plates in the ponds had been buried by sediment.

The ponds in the raster subtraction study were selected because of their proximity to the crevasse splay, where sedimentation rates are typically higher than elsewhere in the study area (Fig. 23). The difference rasters for ponds 1 and 3 show negligible elevation change, with most regions showing values near 0 m of change (Fig. 29). Pond 2 was closest to the crevasse splay; it shows local areas of deposition and erosion, with the small area of erosion located near the toe of the on the steep southern side of the pool and minor deposition near the pool rim (Fig. 29).

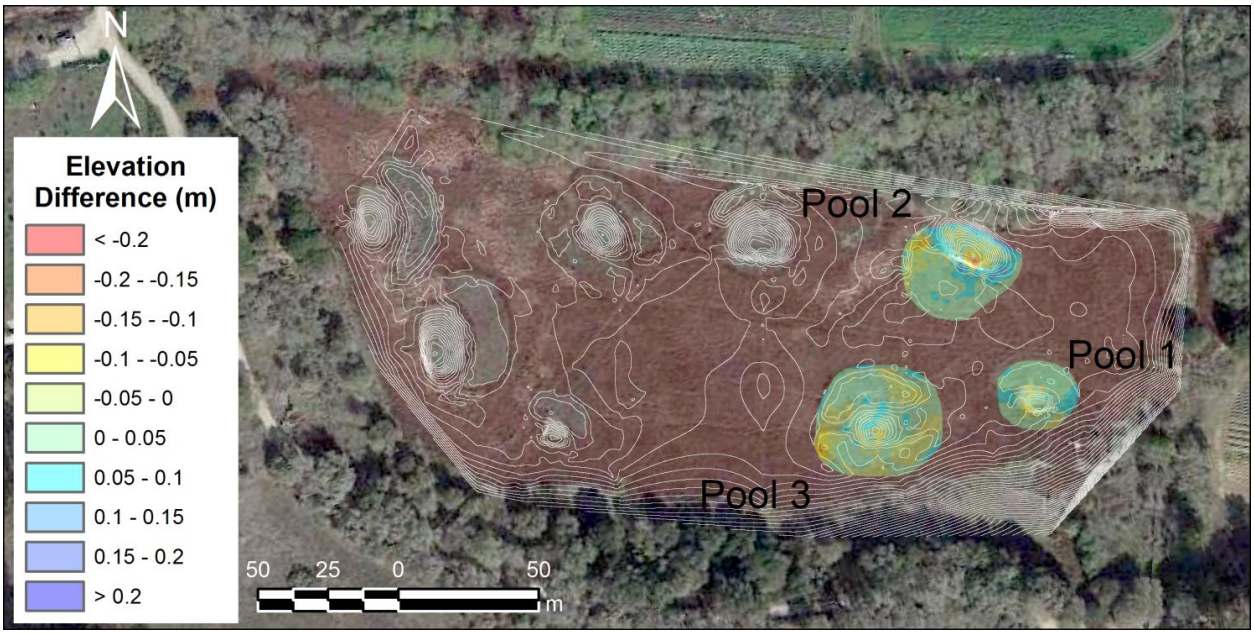

Figure 29: Topographic difference rasters for three ponds in the southern wetland. Topographic contour lines are from preconstruction designs. Contours show pools and adjacent mounds.

3.2.4 Pond staff plates

Given that the excavated ponds may have the highest water residence time of all features in the wetlands, they should trap more suspended sediment than other parts of the floodplain. The annual sediment trapped by each pond in 2014–15 water year, as determined from staff plate burial (Fig. 30), ranged from 0.02 m to 0.05 m (Table 7) with an average depth of 0.03 m. This value is at the edge of detectability in our topographic

surveys. We do not know if the trapped sediment was sourced from outside the ponds or from the pond inner slopes.

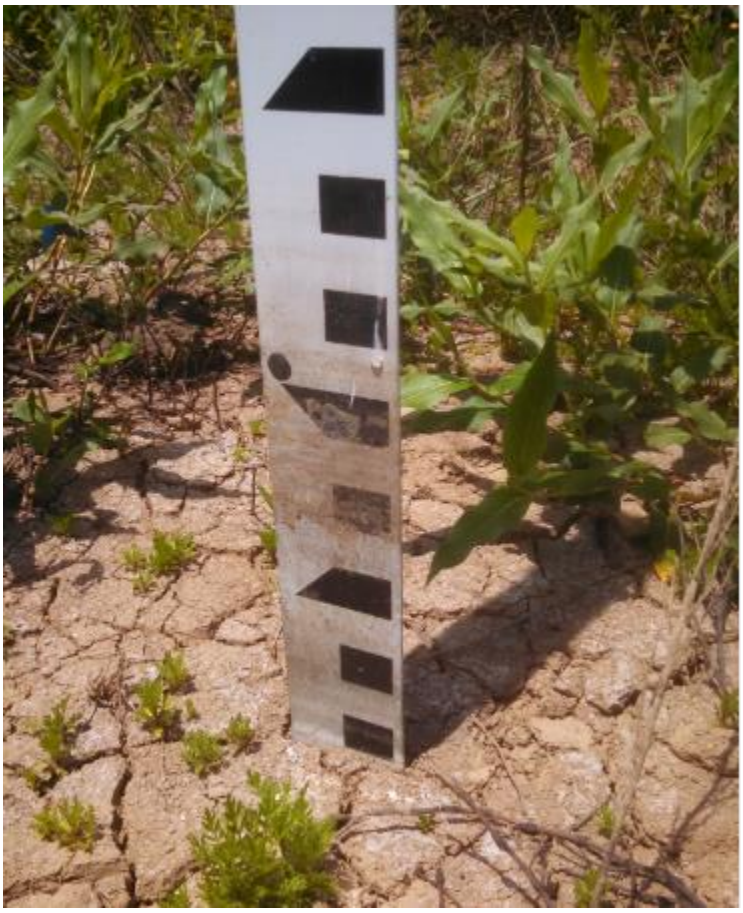

Figure 30: Partial burial of pond staff plate.

Table 7. Sediment depths determined from staff plate readings in each pond.

Pool	Sediment depth (m)
1	0.02
2	0.02
3	0.03
4	0.02
5	0.02
6	0.05
7	0.04
8	0.02
9	0.03
10	0.05

3.3 Sediment trapping with climate change

Climate forecasts for the central California coast are based on past trends and recent modeling studies. The region just north of the Carneros Watershed has become wetter and warmer (minimum temperature) over the last three decades (Flint and Flint 2012). More broadly in California, climate-driven changes include earlier springtime snowmelt and more numerous extended dry periods (Lundquist et al. 2009).

Precipitation models for California are highly spatially variable, with some areas wetter and others dryer (Hughes and Diaz, 2008; Flint and Flint 2012). However, models generally agree that temperature will rise, the dry season will lengthen, and annual precipitation will be concentrated to December and January (Flint and Flint, 2012; Pont et al. 2002). Therefore, it appears that the annual rainfall, whether higher or lower, will be delivered by fewer, but more intense storms during a shorter rain season (Russo et al. 2013). Supporting that general result, strong El Niño events are forecast to double in frequency (Santoso et al. 2013). On the Central California Coast, strong El Niño events are associated with severe winter storms that bring an elevated risk of high rainfall intensity, which fosters high erosion rates on upper slopes, landslides, significant bedload transport events, and large floods (Osterkamp and Friedman 2000; Russo et al. 2013). Both small and large scale storm events are predicted to change in frequency and intensity (Tarasona et al. 2001, Walsh 2004, Sutton and Hodson 2005, Russo et al. 2013). The combination of increased sediment yield and storm runoff with higher peak discharge and runoff volumes will lead to less efficient sediment trapping in the ALBA wetlands by reducing residence time of water parcels (Fig. 19).

3.4 Sediment trapping in the context of future watershed urbanization

Watershed urbanization typically leads to increased impervious cover and expanded storm sewer influence on runoff. The combined effect is to route a higher proportion of each storm directly to stream channels, at the expense of infiltration to groundwater. Modern urban growth typically includes strategies for mitigating some, but not all, of the increased runoff. In turn, increased runoff alters the average sediment retention potential of riparian wetlands and marshes. We altered just the impervious cover variable in a HEC HMS model of the Carneros watershed to assess the future sediment trapping function of ALBA wetlands as a function of watershed impervious cover. Hydrographs were generated for several levels of impervious cover using a series of storms from the month of January 2010 on a HEC HMS model calibrated for the Johnson Bridge gage (Fig. 30). The watershed currently has 4% impervious cover, so it is

approximately represented by the 5% model run in Figure 30. Figures 31 and 32 illustrate the rate at which peak discharge and runoff volume will increase with future impervious cover.

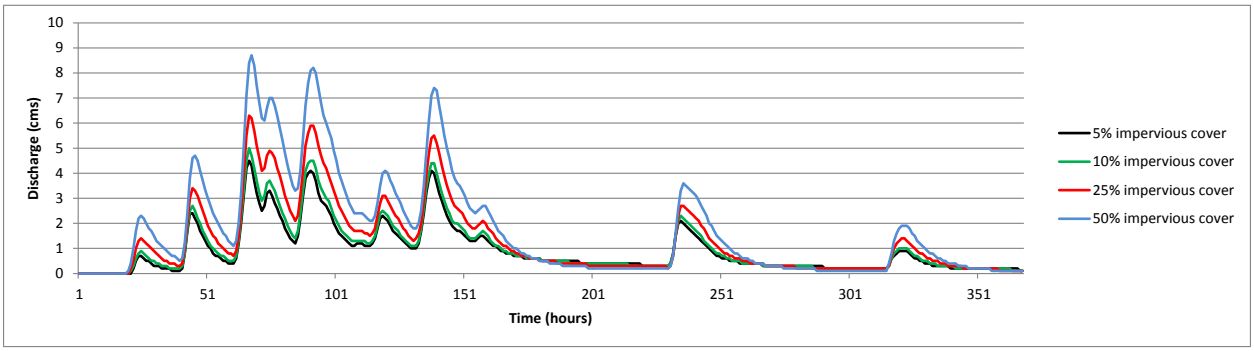

Figure 30: Change in hydrograph over current conditions as a function of % impervious cover in the Carneros Watershed

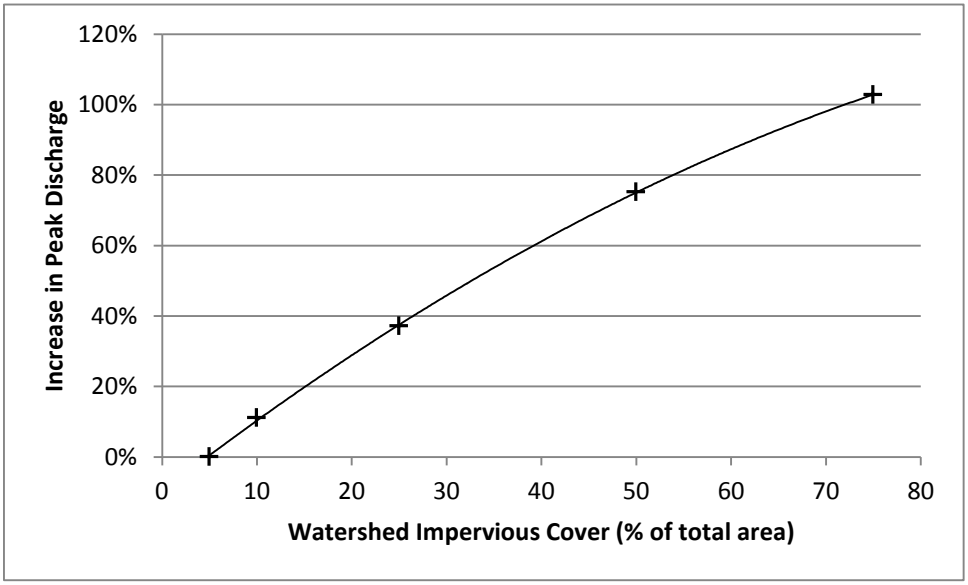

Figure 31: Change in peak discharge over current conditions as a function of % impervious cover in the Carneros Watershed.

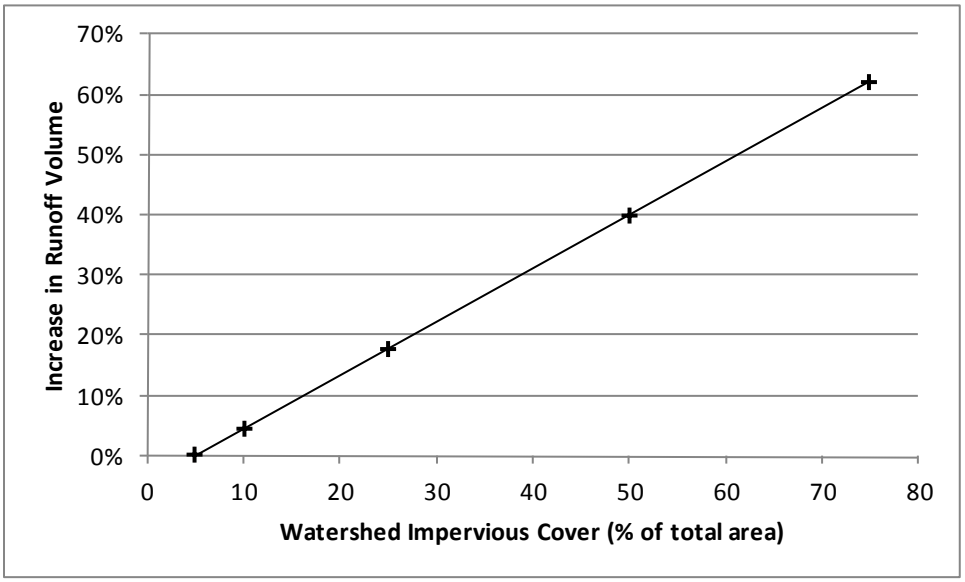

Figure 32: Change in runoff volume over current conditions as a function of % impervious cover in the Carneros Watershed

Given the evidence that increase average discharge decreases residence time, and hence sediment retention potential (Fig. 19), we conclude that future increases in impervious cover would reduce the sediment retention function of the ALBA wetlands.

Currently only 4% of the Carneros Creek's watershed area is impervious, and the other 96% consists of undeveloped land used for agriculture, grazing, or conservation. San Benito County (28% of the watershed) has a well-defined general plan that favors rural, open land and low impact development (San Benito County 2015). Monterey County (72% of the watershed) has zoned the watershed to be chiefly "rural density" residential (5 to 40 ac/unit), and a smaller portion to be "low density" residential (2.5 to 10 ac/unit) (Monterey County 2010). However, Monterey County plans to increase housing density from 5 ac/unit to a range of from1 ac/unit to 0.2 ac/unit on buildable lots, but stopping short of stressing the existing sewer system. While the change in housing density would certainly increase impervious cover, it is beyond the scope of this study to quantify the increase. An increase to 10% would result in a 10% increase in peak discharge (Fig. 31) and a 5% increase in runoff volume (Fig. 32).

The model results support the generally accepted principle that urbanization increases flood magnitudes and runoff volume. However, visual inspection of Figure 30 counters the principle that lag time between storm peaks and peak runoff will diminish as impervious cover increases (Fleming 2007; Hollis, 1975; Hirsch et al. 1990; Leopold,1994; Paul and Meyer 2001; Konrad and Booth 2002; White and Greer 2006).

3.5 Alternative Channel Design Option

A channel was designed to flow through ALBA wetlands, connecting the avulsion point to the Sill Rd. culvert with a meandering channel. The constraints for the channel design included:

1) the available space and site planform geometry,
2) valley slope,
3) floodplain elevation,
4) Sill Rd. culvert invert elevation,
5) the need for frequent flooding (undersized channel) for wetland maintenance,
6) the need to transport sand bedload without aggradation and avulsion (high efficiency)
7) floodplain materials (cohesive clayey soils)

The design has the following bankfull geometry (Table 8; Fig. 33).

Table 8: Bankfull Geometry for Design Channel

English	metric	Feature
	Cross sectional geometry	
28	71	Drainage Area (mi^2, km^2)
58	5.4	Cross sectional area (ft^2, m^2)
8	8	w/d (width to depth ratio)
22	6.6	Width (ft, m)
2.7	0.8	Average depth (ft, m)
28	8.5	Wetted Perimeter (ft, m)
2	0.6	Hydraulic radius (ft, m)
	Planform geometry	
58	18	Radius of curvature (ft, m)
235	72	Meander length (ft, m)
1.5	1.5	Sinuosity
	Longitudinal slope	
0.0009	0.0011	Channel slope
0.0016	0.0016	Valley slope
	Bedload	
	0.30	d50 (median, mm)
	0.45	d84 (84th percentile, mm)

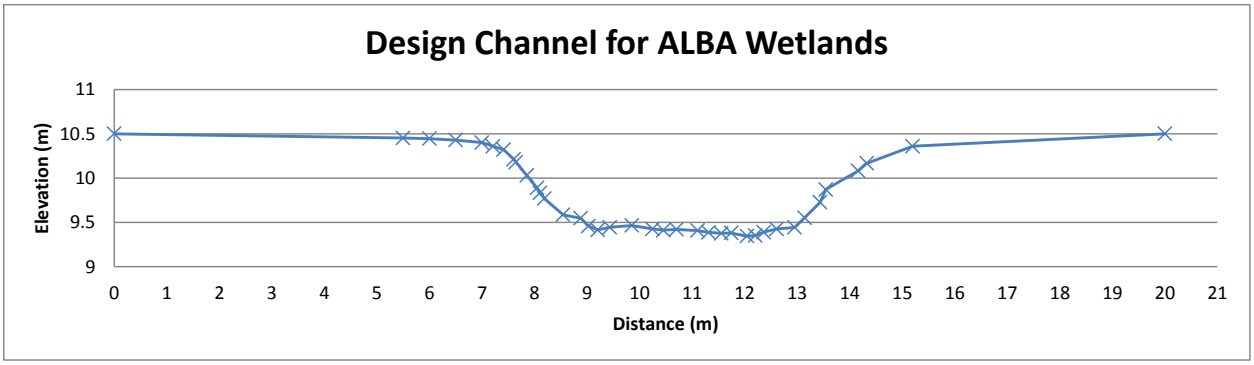

Figure 33: Cross section of a channel with the parameters listed in Table 8.

The design cross sectional area is falls within the scatter of a subset of small, geomorphically-stable channels from the general region (Fig. 34) surveyed by Hecht et al (2013). The planform of the design is plotted in Figure 35. The ponds would have to be filled to allow for natural channel migration across the floodplain.

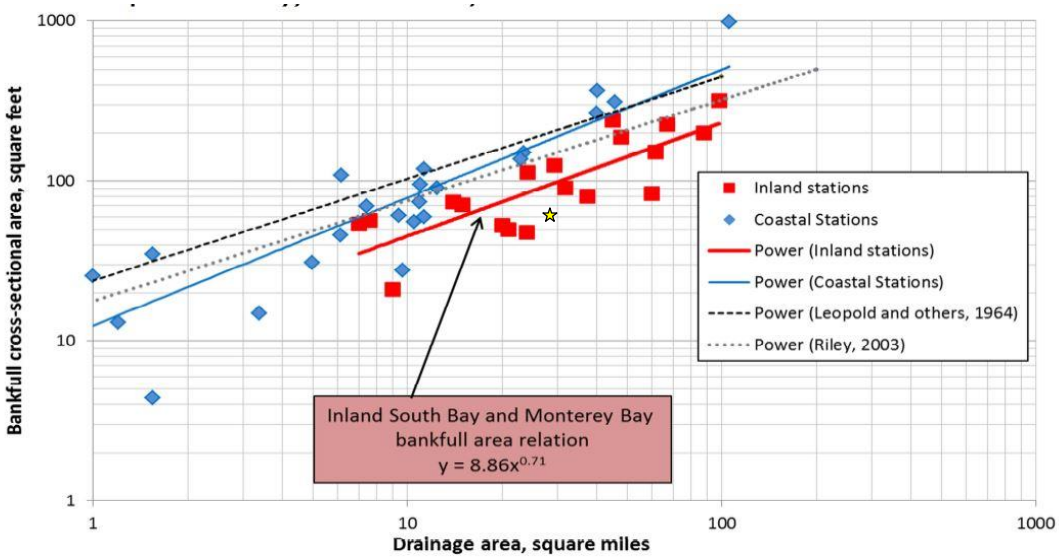

Figure 34: Bankfull cross sectional area (ft^2) as a function of watershed drainage area (mi^2) for a subset of channels in Santa Cruz, Santa Clara Valley, and around Monterey Bay (Hecht et al 2013). Yellow star is the design channel for Carneros Creek.

Figure 35: Approximately-scaled planform of a restored river channel across the southern and northern floodplains using design elements from table 8. Design is plotted on aerial photograph showing pond locations. Depending upon the final channel placement, ponds located near the channel should be decommissioned.

HEC RAS hydraulic modeling using the design channel and a Manning's channel roughness of 0.035, yielded a bankfull discharge of approximately 130 cfs (3.68 cms) (Fig. 36). That discharge has an approximate exceedance recurrence interval of 0.56 years based upon partial duration analysis of a nearby gage (Table 9). Given the flat topography of the site, the floods will have a long flood duration as well. This frequency of flooding and long flood duration will maintain the wetland hydrology and wetland ecosystem currently occupying the northern and southern wetlands. While bedload sediment would be transported down-valley by the channel, a portion of the suspended load would continue to be trapped in the wetlands from overbank flows. The site would continue to aggrade, probably starting with natural levee deposits.

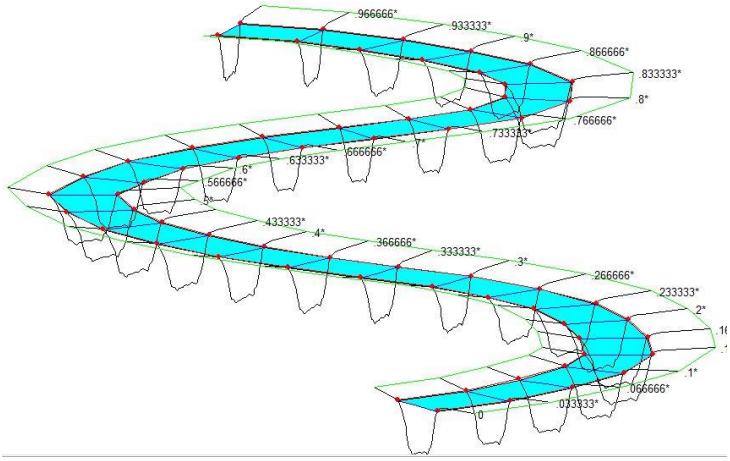

Figure 36: Graphical output of 130 cfs flow reaching bankfull conditions.

Table 9: Partial duration series analysis on 7 years of discharge record at San Miguel Road. Peak flows are determined by San Miguel discharge data scaled by watershed area to Johnson Rd.

Date	Peak (cfs)	Peak_JR (cfs)	Return period (yr)	Annual Exceedance Probability
4/4/2006	440	484	7.00	0.14
1/2/2006	382	420	3.50	0.29
12/21/2001	367	403	2.33	0.43
3/25/2006	259	285	1.75	0.57
3/31/2006	237	261	1.40	0.71
2/25/2004	226	249	1.17	0.86
12/31/2005	205	225	1.00	1.00
1/11/2005	171	188	0.88	1.14
12/31/2004	155	170	0.78	1.29
12/29/2001	143	158	0.70	1.43
12/2/2001	140	154	0.64	1.57
3/17/2006	131	144	0.58	1.71
1/1/2004	115	126	0.54	1.86
12/30/2001	112	123	0.50	2.00
12/29/2003	105	115	0.47	2.14
1/8/2005	104	115	0.44	2.29
1/10/2003	104	115	0.41	2.43
1/2/2002	99	109	0.39	2.57
2/28/2007	95	105	0.37	2.71

Average boundary shear stress (τ_o) far exceeds critical shear stress (τ_c), leaving abundant excess shear to transport the moderately high sand bedload and small pebbles at bankfull conditions (Table 10). If more sediment transport were required, a less sinuous design could be selected.

Table 10: Sediment transport shear stress.

0.055		Dimensionless critical shear (τ^*)
0.40	N/m^2	Critical shear stress (τ_c)
6.6	N/m^2	Average boundary shear stress (τ_o)

HEC RAS modeling output (Table 11) verifies the bankfull geometry input from Table 8, and supports the boundary shear stress value previously calculated as:

$\tau_o = (\gamma w) \times R \times Sc.$

Table 11: Hydraulic and geometry parameters output from HEC RAS at 130 cfs (3.68 cms) discharge in design channel.

5.3	Abkf (m^2)
3.68	Qbkf (m^3/s)
7.8	Wbkf (m)
0.7	Average velocity (m/s)
0.67	R (m)
8.4	WP (m)
6.8	τ_o (N/m^2)

While the channel design presented here is based upon standard geomorphic principles, it should be considered as preliminary and conceptual. A final channel design will require further sediment transport modeling.

4 References

[ESRI] Environmental Systems Resource Institute. 2011. ArcGIS Desktop: Release 10. Redlands, CA.

[IAEA] International Atomic Energy Association. 2005. Fluvial Sediment Transport Analytical Techniques For Measuring Sediment Load. IAEA, Vienna, 2005. IAEA-TECDOC-1461 Printed by the IAEA in Austria, July 2005.

[USDA] Unites States Department of Agriculture. 1996. Forested Wetlands: Functions, Benefits and the Use of Best Management Practices. U.S. Department of Agriculture, Forest Service, Natural Resources Conservation Service, Minnesota. 62 pp.

[CCoWS] Central Coast Watershed Studies. 2004. Protocols for Water Quality and Stream Ecology Research. [Internet]. [Cited 2011 May 5]. Available from: http://ccows.csumb.edu/home/proj/long/protocols/protocols.htm.

[NRCS] 2012 Soil Survey Staff, Natural Resources Conservation Service, United States Department of Agriculture. Soil Survey Geographic (SSURGO) Database for [Monterey County, CA]. Available online at http://soildatamart.nrcs.usda.gov.

[PRISM] PRISM Climate Group, Oregon State University. 2012. http://prism.oregonstate.edu, downloaded 27 Feb 2013.

[USGS] United States Geological Survey. 2006. National land cover database: land-cover. [Internet]. [Cited 2013 February 21]. Available from: http://viewer.nationalmap.gov

Asselman NEM, Middelkoop H. 1995. Floodplain sedimentation: Quantities, patterns and processes. Earth Surface Processes and Landforms 20: 481-499

Bassett, R. 2010. Quantifying spatially-explicit change in sediment storage on an emerging floodplain and wetland on Carneros Creek, CA. CSUMB Senior Thesis in teh Division of Science and Environmental Policy. 27pp.

Bassett, R., in reveiw. Examination of the relative influence of vegetation, distance from inflow, and water depth of sedimentation in a coastal Californian wetland. Draft Masters Thesis in the Division of Science and Environmental Policy, CSU Monterey Bay.

Burnham KP, Anderson DR. 2002. Model Selection and Multi-Model Inference: A practical information-theoretic approach. Second Edition. New York, NY: Springer Science and Business Media, Inc.

Elkhorn Slough National Estuarine Research Reserve, 2007. GIS file downloads available at http://www.elkhornslough.org/GIS/GIS.htm

Elkhorn Slough National Estuarine Research Reserve, 2014. Parsons Slough Project: Annual report to USACE and Regional Water Quality Control Board. Elkhorn Slough National Estuarine Research Reserve, Monterey, CA.

Fleming, S.W. 2007. Quantifying urbanization-associated changes in terrestrial hydrologic system memory. Acta Geophysica 55(3): 359-368.

Flint, L.E., and Flint, A.L. 2012. Simulation of climate change in San Francisco Bay Basins, California: Case studies in the Russian River Valley and Santa Cruz Mountains: U.S. Geological Survey Scientific Investigations Report 2012-5132, 55 p.

Google Inc. 2012. Google Earth (Version 7) [Software]. Available from: http://www.google.com/earth/download/ge/agree.html

Guy HP. 1969. Laboratory Theory and Methods for Sediment Analysis: U.S.Geological Survey, Techniques of Water-Resources Investigations, Book 5, Chapter C1, 58 p.

Guy HP and Norman VW. 1970. Field methods for measurement of fluvial sediment: U.S. Geol. Survey Techniques of Water Resources Inv., bk. 3, chap. C2, 59 p.

Hecht, B., Senter, A., Strudley, M, and Xu, Liang, 2013, New bankfull geometry relations for inland South Bay and Monterey Bay, Central California: Poster presented at 2013 State of the Estuary Conference, Oakland, CA.

Hirsch, R.M., Walker, J.F., Day, J.C., Kallio, R., 1990. The influence of man on hydrologic systems. In: Wolman, W.G., Riggs, H.C. (Eds.), Surfa ce Water Hydrology: The Geology of America, vol. O-1. Geological Society of America, Boulder, CO, USA.

Holland JF, Martin JF, Granata T, Bouchard V, Quigley M, Brown L. 2004. Effects of wetland depth and flow rate on residence time distribution characteristics. Ecological Engineering. 23: 189-203.

Hollis, G.G., 1975. The effects of urbanization on floods of different recurrence intervals. Water Resour. Res. 11, 431-435.

Holloway, R. 2010. Annual sediment retention and hydraulic residence time variability in a riverine wetland receiving unregulated inflow from agricultural runoff. Masters Thesis in the Division of Science and Environmental Policy, CSU Monterey Bay. 72pp.

Hughes, M and Diaz, H. 2008. Climate variability and change in the drylands of Western North America. Global and Planetary Change, v. 64, pp. 111-118.

Kadlec RH, Knight RL. 1996. Treatment Wetlands. CRC Press, New York.

Kilpatrick FA, Wilson JF. 1989. Measurement of time of travel in streams by dye tracing. Techniques of Water-Resources Investigations of the United States Geological Survey, Chapter A9.

Konrad, C.P., Booth, D.B., 2002. Hydrologic trends associated with urban development for selected streams in the Puget Sound Basin, Western Washington. U.S. Geological Survey, Water-Resources Investigations Report 02-4040. Tacoma, WA, USA.

Largay B. 2007. ALBA Triple M wetlands restoration project. Existing conditions and conceptual design technical advisory committee review draft. Largay Hydrologic Sciences, LCC

Laurel Marcus and Associates. 2003. Triple M Ranch Land Management Plan. Prepared for Elkhorn Slough Foundation.

Leopold, L.B., 1994. A View of the River. Harvard University Press, Cambridge, MA, USA.

Leopold, L. and Wolman, G. 1960. River meanders. Geological Society of America Bulletin, v.71, pp.769-793.

Lundquist, J.D., Dettinger, M.D., Stewart, I.T., and Cayan, D.R., 2009, Variability and trends in spring runoff in the western United States, chap. 5 in Environmental effects: Twentieth-century observations and twenty-first century projections, Part II. of Wagner, Frederic, ed., 2009, Climate warming in western North America—Evidence and environmental effects: Salt Lake City, Utah, University of Utah Press, p. 63-76.

Monterey County. 2010. Monterey County General Plan, North County Area Plan [Internet]. Monterey County: Board of Supervisors and Planning Commission. [cited 2015 Aug 8].

Osterkamp, W. R., and Friedman J. M. 2000. The disparity between extreme rainfall events and rare floods – with emphasis on the semi-arid American West. Hydrolog. Process., 14, 2817-2829, doi:10.1002/1099-1085(200011/12)14:16/17<2817::AID-HYP121>3.0.CO;2-B.

Paul, M.J., Meyer, J.L., 2001. Streams in the urban landscape. Ann. Rev. Ecol. Syst. 32, 333-365.

Pont, D., J. Day, P. Hensel, E. Franquet, F. Torre, P. Rioual, C. Ibañez, and E. Coulet. 2002. Response scenarios for the deltaic plain of the Rhône in the face of an acceleration in the rate of sea level rise, with a special attention for Salicornia-type environments. Estuaries 25: 337-358.

PRISIM Climate Group, Oregon State Univertiy, http://www.prisimclimate.org, created 4th Feb, 2004

R Development Core Team (2010). R: A language and environment for statistical computing. R Foundation for Statistical Computing, Vienna, Austria. ISBN 3-900051-07-0, URL http://www.R-project.org

Raines, Mellon and Carella Inc. 2002. Revised Basin Management Plan. Pajaro Valley Water Management Agency: Watsonville, CA.

Rosenberg, L., 2001, Geologic Resources and Constraints, Monterey County, California: A Technical Report for the Monterey County 21st Century General Plan Update Program, prepared for County of Monterey Environmental Resource Policy Department, pp. 91.

Russo, T. A., Fisher, A. T., and Winslow, D. M. 2013. Regional and local increases in storm intensity in the San Francisco Bay Area, USA, between 1890 and 2010. J. Geophys. Res. Atmos., 118, doi:10.1002/jgrd.50225.

San Benito County. 2015. 2035 General Plan. [Internet]. San Benito County: Board of Supervisors. [cited 2015 Aug 8].

Santoso A, McGregor S, Jin FF, Cai W, England MH, An SI, McPhaden MJ, Guilyardi E. 2013. Late-twentieth -century emergence of the El Nino propagation asymmetry and future projections. Nature 504, 126-30

Smith, D.P., Diehl, T., Turrini-Smith, L.A., Maas-Baldwin, J, and Croyle, Z., 2009, River restoration strategies within channelized, low-gradient landscapes of West Tennessee, USA; in James, A., Rathburn, S., and Whittecar, R., eds, Management and Restoration of Fluvial Systems with Broad Historical Changes and Human Impacts: Geological Society of America Special Paper 451., p. 215-229.

Soil Conservation Service. 1978. Soil survey of Monterey County, California. United States Department of Agriculture: Salinas, CA. p. 228.

Steiger J, Gurnell AM, Petts GE. 2001. Sediment deposition along the channel margins of a reach of the middle river Severn, UK. Regulated Rivers: Research and Management 17: 443-460.

Stern DA, Khanbilvardi R, Alair JC, Richardson W. 2001. Description of flow through a natural wetland using dye tracer tests. Ecological Engineering. 18: 173-184.

Sutton, R.T., and D.L.R. Hodson. 2005. Atlantic Ocean forcing and North American and European summer climate. Science 309: 115-118.

Tarasona, J., W. E. Arntz and E. C. Maruenda (eds.) 2001. El Niño en América Latina: Impactos Biológicos y Sociales. El Niño in Latin America: Biologic and Social Impacts. Consejo Nacional de Ciencia y Tecnología, Lima, Perú. 423 pp.

Walsh, K. 2004. Tropical cyclones and climate change: unresolved issues. Climate Research 27: 77-83.

White, M.D., Greer, K.A. 2006. The effects of watershed urbanizations on the stream hydrology and riparian vegetation of Los Penasquitos Creek, California. Landscape and Urban Planning 74: 125-138.

Wilson JF, Cobb ED, Kilpatrick FA.1986. Fluorometric procedures for dye tracing. Book 3, Chapter Al2. Applications of hydraulics. Revised Techniques of Water-Resources Investigations of the United States Geological Survey. Department of the United States Government Printing Office, Washington: 1986.

5 Appendix A: Turf Mat Data

Mat ID	Elev (m)	Veg Mass	Vegetation Type	Dist from Inflow (m)	Dry Sed w/ Organics (g)	Trapped Sediment (g)	Normalized Trapped Sediment (g m^{-2})
A1	1.967	3.114	Polygonum	183.9	41.1	32.5	360.7
A2	2.109	4.085	Polygonum	165.9	38.2	29.8	331.3
A3	2.170	3.832	Polygonum	147.7	84.7	66.5	739.4
A4	2.170	5.708	Polygonum	136.0	55.8	46.9	520.8
A5	2.415	3.594	Polygonum	128.8	65.5	56.4	627.2
B1	2.091	4.752	Polygonum	153.2	47.0	39.2	435.3
B2	2.153	3.928	Polygonum	133.3	52.7	41.6	462.0
B3	2.257	3.649	Polygonum	115.1	48.6	42.7	474.3
B4	2.199	4.937	Polygonum	103.3	102.6	90.5	1005.6
B5	2.513	3.493	Polygonum	100.0	38.8	34.7	386.0
C1	2.079	5.562	Polygonum	146.3	37.0	30.6	339.7
C2	1.971	3.401	Polygonum	124.3	49.1	41.9	465.8
C3	2.287	4.307	Polygonum	102.5	70.8	61.6	684.1
C4	2.269	4.734	Polygonum	81.3	104.1	90.7	1007.6
C5	2.304	2.751	Reed	69.9	160.3	144.1	1600.8
D1	2.221	3.658	Polygonum	123.0	76.0	65.6	728.7
D2	2.374	1.829	Polygonum	94.4	83.8	72.7	807.9
D3	2.385	3.747	Polygonum	68.6	60.4	51.8	575.5
D4	2.322	4.258	Polygonum	49.8	112.4	100.5	1116.6
D5	2.212	0.581	Polygonum	40.0	167.4	149.9	1665.1
DT1	1.461	0.188	Polygonum	154.3	214.6	184.8	2053.7
DT2	1.378	1.155	Polygonum	186.3	288.5	258.8	2875.2
E1	2.122	2.02	Reed	18.4	288.3	255.7	2841.4
F1	2.580	1.446	Reed	90.1	119.0	106.1	1178.9
F2	2.464	0.744	Reed	119.6	171.0	147.8	1642.8
F3	2.374	1.976	Polygonum	149.6	208.9	183.1	2034.9
F4	2.348	1.906	Polygonum	178.4	41.3	34.5	382.8
G1	2.478	5.707	Polygonum	193.1	210.1	178.2	1980.2
G2	2.364	7.084	Polygonum	164.2	58.0	49.5	549.8

G3	2.524	2.437	Reed	134.5	101.3	88.2	980.4
G4	2.494	5.53	Polygonum	104.3	154.1	135.5	1505.4
G6	2.772	3.171	Polygonum	48.3	87.1	80.4	893.0
G7	2.537	1.774	Reed	25.1	206.1	189.5	2105.4
G8	2.740	3.638	Polygonum	26.9	186.0	172.5	1916.8
G9	2.672	-	Polygonum	51.9	109.0	100.5	1116.4
G10	2.503	-	Polygonum	82.3	118.7	105.1	1167.9
H1	2.261	3.15	Polygonum	179.7	96.8	65.2	724.3
H2	2.417	3.15	Polygonum	150.9	53.1	45.0	499.9
H3	2.458	4.567	Polygonum	123.5	105.8	93.0	1033.1
H4	2.714	3.061	Polygonum	96.6	50.0	45.2	501.8
H5	2.640	3.335	Polygonum	73.9	141.5	129.1	1434.8
H6	2.642	2.183	Polygonum	54.2	247.0	223.8	2486.2
H7	2.663	3.465	Polygonum	47.1	76.0	69.2	769.2
H9	2.610	3.604	Polygonum	79.2	53.8	48.3	536.6
H10	2.700	4.188	Polygonum	106.0	32.6	24.4	271.1
I1	2.411	2.956	Polygonum	178.5	99.8	89.1	990.1
I2	2.349	2.869	Polygonum	153.7	89.8	77.6	862.1
I3	2.483	4.048	Polygonum	129.2	138.4	122.3	1359.3
I4	2.517	2.83	Polygonum	105.4	127.0	110.4	1226.7
I5	2.638	3.637	Polygonum	90.4	134.8	119.5	1327.7
I6	2.582	2.384	Polygonum	78.8	141.4	127.0	1411.5
I7	2.603	3.048	Polygonum	79.1	65.6	57.9	643.5
I8	2.828	2.462	Polygonum	91.9	25.9	22.9	254.0
I9	3.095	2.053		108.9	0	0	0
J1	3.016	3.619		120.4	0	0	0
J2	2.963	2.358		109.6	0	0	0